Supporting Information

Figure S1 Schematic representation of the isobologram of Steel and Peckham. Envelope of additivity, surrounded by Mode I (solid line) and Mode II (dotted lines) isobologram lines, was constructed from the dose-response curves of bendamustine and a combined drug. The concentrations that produced 80% or 50% growth inhibition were expressed as 1.0 on the ordinate and the abscissa of isobolograms. Combined data points Pa, Pb, Pc and Pd represent supra-additive, additive, sub-additive and protective effects, respectively.
(TIF)

Figure S2 Time-course analysis of ATM, ATR and p53 phosphorylation in HBL-2 cells treated with IC50 values of bendamustine or 4-OHCY. We used specific antibodies against phosphorylated p53 at Ser-15, phosphorylated ATM at Ser-1981 and phosphorylated ATR at Ser-428 (Cell Signaling Technology). The membranes were reblotted with anti-GAPDH antibody to serve as an internal control.
(TIF)

Acknowledgments

The authors are indebted to Professor Martin J.S. Dyer (MRC Toxicology Unit, Leicester University, Leicester, UK) for providing Granta 519 and NCEB-1 cell lines.

Author Contributions

Conceived and designed the experiments: NH JK YK YF. Performed the experiments: NH JK TY DK TW MU MA YK YF. Analyzed the data: NH JK TY DK TW TU YK YF. Contributed reagents/materials/analysis tools: SM YN. Wrote the paper: NH JK TY TU YK YF.

References

1. Tageja N, Nagi J (2010) Bendamustine: something old, something new. Cancer Chemother Pharmacol 66: 413–423.
2. Hartmann M, Zimmer C (1972) Investigation of cross-link formation in DNA by the alkylating cytostatic IMET 3106, 3393 and 3943. Biochim Biophys Acta 287: 386–389.
3. Strumberg D, Harstrick A, Doll K, Hoffmann B, Seeber S (1996) Bendamustine hydrochloride activity against doxorubicin-resistant human breast carcinoma cell lines. Anticancer Drugs 7: 415–421.
4. Leoni LM, Bailey B, Reifert J, Bendall HH, Zeller RW, et al. (2008) Bendamustine (Treanda) displays a distinct pattern of cytotoxicity and unique mechanistic features compared with other alkylating agents. Clin Cancer Res 14: 309–317.
5. Schwänen C, Hecker T, Hübinger G, Wölfle M, Ritgen W, et al. (2002) In vitro evaluation of bendamustine induced apoptosis in B-chronic lymphocytic leukemia. Leukemia 16: 2096–2105.
6. Roué G, López-Guerra M, Milpied P, Pérez-Galán P, Villamor N, et al. (2008) Bendamustine is effective in p53-deficient B-cell neoplasms and requires oxidative stress and caspase-independent signaling. Clin Cancer Res 14: 6907–6915.
7. Beeharry N, Rattner JB, Bellacosa A, Smith MR, Yen TJ (2012) Dose dependent effects on cell cycle checkpoints and DNA repair by bendamustine. PLoS ONE 7: e40342.
8. Knauf WU, Lissichkov T, Aldaoud A, Liberati A, Loscertales J, et al. (2009) Phase III randomized study of bendamustine compared with chlorambucil in previously untreated patients with chronic lymphocytic leukemia. J Clin Oncol 27: 4378–4384.
9. Friedberg JW, Cohen P, Chen L, Robinson KS, Forero-Torres A, et al. (2008) Bendamustine in patients with rituximab-refractory indolent and transformed non-Hodgkin's lymphoma: results from a phase II multicenter, single-agent study. J Clin Oncol 26: 204–210.
10. Robinson KS, Williams ME, van der Jagt RH, Cohen P, Herst JA, et al. (2008) Phase II multicenter study of bendamustine plus rituximab in patients with relapsed indolent B-cell and mantle cell non-Hodgkin's lymphoma. J Clin Oncol 26: 4473–4479.
11. Rummel MJ, Niederle N, Maschmeyer G, Banat GA, von Grünhagen U, et al. (2013) Bendamustine plus rituximab versus CHOP plus rituximab as first-line treatment for patients with indolent and mantle-cell lymphomas: an open-label, multicetre, randomised, phase 3 non-inferiority trial. Lancet 381: 1203–1210.
12. Ohmachi K, Niitsu N, Uchida T, Kim SJ, Ando K, et al. (2013) Multicenter phase II study of bendamustine plus rituximab in patients with relapsed or refractory diffuse large B-cell lymphoma. J. Clin Oncol 31: 2103–2109.
13. McCloskey JK, Broome CM, Cheson BD (2013) Safe and effective treatment of aggressive non-Hodgkin lymphoma with rituximab and bendamustine in patients with severe liver impairment. Clin Adv Hematol Oncol 11: 184–188.
14. Hitz F, Fisher N, Pabst Th, Casper C, Berthod G, et al. (2013) Rituximab, bendamustine, and lenalidomide in patients with aggressive B cell lymphoma not eligible for high-dose chemotherapy or anthracycline-based therapy: phase I results of the SAKK 38/08 trial. Ann Hematol 92: 1033–1040.
15. Lentzsch S, O'Sullivan A, Kennedy RC, Abbas M, Dai L, et al. (2012) Combination of bendamustine, lenalidomide, and dexamethasone (BLD) in patients with relapsed or refractory multiple myeloma is feasible and highly effective: results of phase 1/2 open-label, dose escalation study. Blood 119: 4608–4613.
16. Offidani M, Corvatta L, Maracci L, Liberati AM, Ballanti S, et al. (2013) Efficacy and tolerability of bendamustine, bortezomib and dexamethasone in patients with relapsed-refractory multiple myeloma: a phase II study. Blood Cancer J 3: e162.
17. Damaj G, Gressin R, Bouabdallah K, Cartron G, Choufi B, et al. (2013) Results from a prospective, open-label, phase II trial of bendamustine in refractory or relapsed T-cell lymphomas: the BENTLY trial. J Clin Oncol 31: 104–110.
18. Köster W, Stamatis G, Heider A, Avramidis K, Wilke H, et al. (2004) Carboplatin in combination with bendamustine in previously untreated patients with extensive-stage small cell lung cancer (SCLC). Clin Drug Investig 24: 611–618.
19. Layman RM, Ruppert AS, Lynn M, Mrozek E, Ramaswamy B, et al. (2013) Severe and prolonged lymphopenia observed in patients treated with bendamustine and erlotinib for metastatic triple negative breast cancer. Cancer Chemother Pharmacol 71: 1183–1190.
20. Chow KU, Boehrer S, Geduldig K, Krapohl A, Hoelzer D, et al. (2001) *In vitro* induction of apoptosis of neoplastic cells in low-grade non-Hodgkin's lymphomas using combinations of established cytotoxic drugs with bendamustine. Haematologica 86: 485–493.
21. Chow KU, Noval D, Boehrer S, Ruthardt M, Knau A, et al. (2003) Synergistic effects of chemotherapeutic drugs in lymphoma cells are associated with down-regulation of inhibitor of apoptosis proteins (IAPs), prostate-apoptosis-response-gene 4 (Par-4), death-associated protein (Daxx) and with enforced caspase activation. Biochem Pharmacol 66: 711–724.
22. Castegnaro S, Visco C, Chieregato K, Bernardi M, Albiero E, et al. (2012) Cytosine arabinoside potentiates the apoptotic effect of bendamustine on several B- and T-cell leukemia/lymphoma cells and cell lines. Leuk Lymphoma 53: 2262–2258.
23. Visco C, Castegnaro S, Chieregato K, Bernardi M, Albiero E, et al. (2012) The cytotoxic effects of bendamustine in combination with cytarabine in mantle lymphoma cell lines. Blood Cell Mol Dis 48: 68–75.
24. Cai B, Lyu H, Huang J, Wang S, Lee CK, et al. (2013) Combination of bendamustine and entinostat synergistically inhibits proliferation of multiple myeloma cells via induction of apoptosis and DNA damage response. Cancer Lett 335: 343–350.
25. Koenigsmann M, Knauf W, Herold M, Pasold R, Müller G, et al. (2004) Fludarabine and bendamustine in refractory and relapsed indolent lymphoma - multicenter phase I/II trial of the East German Society of Hematology and Oncology (OSHO). Leuk Lymphoma 45: 1821–1827.
26. Weide R, Hess G, Köppler H, Heymanns J, Thomalla J, et al. (2007) German Low Grade Lymphoma Study Group: High anti-lymphoma activity of bendamustine/mitoxantrone/rituximab in rituximab pretreated relapsed or refractory indolent lymphomas and mantle cell lymphomas. A multicenter phase II study of the German Low Grade Lymphoma Study Group (GLSG). Leuk Lymphoma 48: 1299–1306.
27. Visco C, Finotto S, Zambello R, Paolini R, Menin A, et al. (2013) Combination of rituximab, bendamustine, and cytarabine for patients with mantle-cell non-Hodgkin lymphoma ineligible for intensive regimens or autologous transplantation. J Clin Oncol 31: 1442–1449.
28. Visco C, Finotto S, Pomponi F, Sartoli R, Laveder F, et al. (2013) The combination of rituximab, bendamustine, and cytarabine for heavily pretreated relapsed/refractory cytogenetically high-risk patients with chronic lymphocytic leukemia. Am J Hematol 88: 289–293.
29. Abe M, Nozawa Y, Wakasa H, Ohno H, Fukuhara S (1988) Characterization and comparison of two newly established Epstein-Barr virus-negative lymphoma B-cell lines. Surface markers, growth characteristics, cytogenetics, and transplantability. Cancer 61: 483–490.
30. Hiraoka N, Kikuchi J, Koyama D, Wada T, Mori S, et al. (2013) Alkylating agents induce histone H3K18 hyperacetylation and potentiate HDAC inhibitor-mediated global histone acetylation and cytotoxicity in mantle cell lymphoma. Blood Cancer J 3: e169.
31. Furukawa Y, Vu HA, Akutsu M, Odgerel T, Izumi T, et al. (2007) Divergent cytotoxic effects of PKC412 in combination with conventional antileukemic

agents in FLT3 mutation-positive versus -negative leukemia cell lines. Leukemia 21: 1005–1014.
32. Koyama D, Kikuchi J, Hiraoka N, Wada T, Kurosawa H, et al. (2014) Proteasome inhibitors exert cytotoxicity and increase chemosensitivity via transcriptional repression of Notch1 in T-cell acute lymphoblastic leukemia. Leukemia, advanced online publication, 17 January 2014; doi:10.1038/leu.2013.366.
33. Wright AMP, Gati WP, Paterson ARP (2000) Enhancement of retention and cytotoxicity of 2-chlorodeoxyadenosine in cultured human leukemic lymphoblasts by nitrobenzylthioinosine, an inhibitor of equilibrative nucleoside transport. Leukemia 14: 52–60.
34. Kikuchi J, Yamada S, Koyama D, Wada T, Nobuyoshi M, et al. (2013) The novel orally active proteasome inhibitor K-7174 exerts anti-myeloma activity *in vitro* and *in vivo* by down-regulating the expression of class I histone deacetylases. J Biol Chem 288: 25593–25602.
35. Yamauchi T, Negoro E, Kishi S, Takagi K, Yoshida A, et al. (2009) Intracellular cytarabine triphosphate production correlates to deoxycytidine kinase/cytosolic 5′-nucleotidase II expression ratio in primary acute myeloid leukemia cells. Biochem Pharmacol 77: 1780–1786.
36. Yamauchi T, Ueda T (2005) A sensitive new method for clinically monitoring cytarabine concentrations at the DNA level in leukemia cells. Biochem Pharmacol 69: 1795–1803.
37. Yamauchi T, Ueda T, Nakamura T (1996) A new sensitive method for determination of intracellular 1-β-D-arabinofuranosylcytosine 5′-triphosphate content in human materials *in vivo*. Cancer Res 56: 1800–1804.
38. Rasschaert M, Schrijvers D, Van den Brande J, Dyck J, Bosmans J, et al. (2007) A phase I study of bendamustine hydrochloride administered day 1+2 every 3 weeks in patients with solid tumours. Br J Cancer 96: 1692–1698.
39. Ogura M, Uchida T, Taniwaki M, Ando K, Watanabe T, et al. (2010) Phase I and pharmacokinetic study of bendamustine hydrochloride in relapsed or refractory indolent B-cell non-Hodgkin lymphoma and mantle cell lymphoma. Cancer Sci 101: 2054–2058.
40. Hill BT (1972) Studies on the transport and cellular distribution of chlorambucil in the Yoshida ascites sarcoma. Biochem Pharmacol 21: 495–502.
41. Boyd VL, Robbins JD, Egan W, Ludeman SM (1986) ^{31}P nuclear magnetic resonance spectroscopic observation of the intracellular transformations of oncostatic cyclophosphamide metabolites. J Med Chem 29: 1206–1210.
42. Pastor-Anglada M, Molina-Arcas M, Casado FJ, Bellosillo B, Colomer D, et al. (2004) Nucleoside transporters in chronic lymphocytic leukemia. Leukemia 18: 385–393.
43. Fernandez-Calotti PX, Colomer D, Pastor-Anglada M (2011) Translocation of nucleoside analogs across the plasma membrane in hematologic malignancies. Nucleosides, Nucleotides and Nucleic Acids 30: 1324–1340.
44. Staib P, Schinköthe T, Dimski T, Lathan B, Boos J, et al. (1999) In-vitro modulation of Ara-CTP accumulation in fresh AML cells by bendamustine in comparison with fludarabine, 2-CDA and gemcitabine. Blood 94: 63a.
45. Gandhi V, Estey E, Keating MJ, Chucrallah A, Plunkett W (1996) Chlorodeoxyadenosine and arbinosylcytosine in patients with acute myelogenous leukemia: Pharmacokinetic, pharmacodynamic, and molecular interactions. Blood 87: 256–264.
46. Chow KU, Boehrer S, Napieralski S, Novak D, Knau A, et al. (2003) In AML cell lines Ara-C combined with purine analogues is able to exert synergistic as well as antagonistic effects on proliferation, apoptosis and disruption of mitochondrial membrane potential. Leuk Lymphoma 44: 165–173.
47. Petersen AJ, Brown RD, Gibson J, Pope B, Luo XF, et al. (1996) Nucleoside transporters, bcl-2 and apoptosis in CLL cells exposed to nucleoside analogues *in vitro*. Eur J Haematol 56: 213–220.
48. Chan KK, Hong PS, Tutsch K, Trump DL (1994) Clinical pharmacokinetics of cyclophosphamide and metabolites with and without SR-2508. Cancer Res 54: 6421–6429.
49. Herold M, Schulze A, Niederwieser D, Franke A, Fricke HJ, et al. (2006) Bendamustine, vincristine and prednisone (BOP) versus cyclophosphamide, vincristine and prednisone (COP) in advanced indolent non-Hodgkin's lymphoma and mantle cell lymphoma: results of a randomised phase III trial (OSHO# 19). J Cancer Res Clin Oncol 132: 105–112.
50. Visani G, Malerba L, Stefani PM, Capria S, Galieni P, et al. (2011) BeEAM (bendamustine, etoposide, cytarabine, melphalan) before autologous stem cell transplantation is safe and effective for resistant/relapsed lymphoma patients. Blood 118: 3419–3425.

Int J Hematol (2014) 99:726–736
DOI 10.1007/s12185-014-1573-3

ORIGINAL ARTICLE

Suitable drug combination with bortezomib for multiple myeloma under stroma-free conditions and in contact with fibronectin or bone marrow stromal cells

Jiro Kikuchi · Daisuke Koyama · Harumi Y. Mukai · Yusuke Furukawa

Received: 23 December 2013 / Revised: 17 March 2014 / Accepted: 17 March 2014 / Published online: 6 April 2014

Abstract Several clinical trials have demonstrated the effectiveness of bortezomib in combination with various anti-myeloma agents; however, no definitive information is available regarding drugs best suited for use in combination with bortezomib. Using isobologram analysis, we investigated the combined effects of bortezomib with four key anti-myeloma drugs (melphalan, cyclophosphamide, doxorubicin and lenalidomide), which represent components of major bortezomib-based regimens with corticosteroids, in three myeloma cell lines (U266, RPMI8226 and KMS-12BM) under various conditions. Melphalan showed the best performance with bortezomib under all culture conditions tested (liquid culture, on fibronectin-coated plates, and co-culture with bone marrow stromal cells), whereas cyclophosphamide was antagonistic with bortezomib especially in the presence of stromal cells. Doxorubicin showed additive effects under stroma-free conditions and in contact with fibronectin, but was rather antagonistic in the presence of stromal cells. In contrast, lenalidomide exerted the most favorable effect with bortezomib in contact with stromal cells. Consistent with these results, caspase-3 was activated more strongly by melphalan than by other agents in combination with bortezomib. Moreover, bortezomib-induced up-regulation of CHOP was readily enhanced by lenalidomide in contact with stromal cells. The present findings may provide fundamental information for the selection of bortezomib-based regimens for myeloma patients.

Keywords Bortezomib · Drug combination · Isobologram · Bone marrow microenvironment

J. Kikuchi · D. Koyama · Y. Furukawa (✉)
Division of Stem Cell Regulation, Center for Molecular Medicine, Jichi Medical University, 3311-1 Yakushiji, Shimotsuke, Tochigi 329-0498, Japan
e-mail: furuyu@jichi.ac.jp

H. Y. Mukai
Medical Affairs Division, Janssen Pharmaceutical K.K., 3-5-1 Nishi-Kanda, Chiyoda-ku, Tokyo 101-0065, Japan

Introduction

Bortezomib (Velcade®) is the first proteasome inhibitor approved for clinical application and now indispensable for the treatment of multiple myeloma (MM) [1, 2]. The proteasome is a proteolytic machinery that executes the degradation of polyubiquitinated proteins to maintain cellular homeostasis [3]. MM cells are very sensitive to proteotoxic stress because of intracellular protein overload due to excessive immunoglobulin synthesis, rapid cell cycling, and inhibition of proteolytic apoptosis signaling, providing a rationale for therapeutic intervention [4]. Indeed, we and others have demonstrated that bortezomib increases proteotoxic stress via down-regulation of histone deacetylases (HDACs) [5–7]. In addition, this drug can overcome cell adhesion-mediated drug resistance (CAM-DR) via down-regulation of very late antigen-4 (VLA-4) in an HDAC-dependent manner [8–10].

From the results of mechanistic studies, it is easy to speculate that bortezomib could sensitize MM cells to other anti-cancer agents, because HDACs play crucial roles in the innate drug resistance of cancer stem cells [11] and VLA-4-mediated CAM-DR is a major cause of treatment failure in MM [12, 13]. In fact, bortezomib-based regimens have been established as primary options for both transplantation-eligible and -ineligible patients with MM. Considerable clinical benefits have been obtained by VMP (Velcade® with melphalan and prednisone) [14], VCD

(Velcade® with cyclophosphamide and dexamethasone) [15], VTD (Velcade® with thalidomide and dexamethasone) [16], RVd (Velcade® with lenalidomide [Revlimid®] and dexamethasone) [17], PAD (bortezomib with pegylated liposomal doxorubicin and dexamethasone) [18] and several other combinations in independent studies. The emerging question is which is the best regimen as a first-line treatment; however, it is not realistic to determine the superiority among these regimens on the basis of clinical trials.

Preclinical investigation is, therefore, important to define the most suitable bortezomib combination to further improve the treatment outcome of patients with MM; however, to our knowledge, no systematic studies have been conducted on this subject. In this study, we attempted to determine the optimal agents to be combined with bortezomib using isobologram analyses not only under the usual stroma-free conditions but also in contact with fibronectin and bone marrow (BM) stromal cells, because the interaction with stromal cells and/or the extracellular matrix promotes the survival, proliferation and drug resistance of MM cells [19, 20]. The present study may provide a rationale for the design of effective bortezomib-based regimens for myeloma patients.

Materials and methods

Drugs

The drugs used in this study and their sources are bortezomib (LC Laboratories, Wobum, MA, USA), 4-Hydroxycyclophosphamide (4-OHCY; an active form of cyclophosphamide), melphalan (L-PAM), dexamethasone (Wako Biochemicals, Osaka, Japan), doxorubicin (Meiji, Tokyo, Japan) and lenalidomide (BioVision, Milpitas, CA, USA). All drugs were dissolved in dimethyl sulfoxide at appropriate concentrations and used at a final dilution of 1/1000. The final concentration of dimethyl sulfoxide in the culture medium was <0.1 %, a concentration that did not affect the drug effects and cell growth per se.

Cells and cell culture

We used 3 *bona fide* human MM cell lines, KMS12-BM, RPMI8226 and U266, in this study [21]. Other hematopoietic cell lines and their origins are IM9 (Epstein-Barr virus-immortalized B-lymphoblastoid cells), MOLT-3 (acute T-lymphoblastic leukemia), and HBL-2 (mantle cell lymphoma). These cell lines were purchased from the Health Science Research Resources Bank (Osaka, Japan) and maintained in RPMI1640 medium (Sigma-Aldrich, St. Louis, MO, USA) supplemented with 10 % heat-inactivated fetal calf serum (FCS) (Sigma-Aldrich). The human BM-derived stromal cell line UBE6T-7, which was immortalized by transducing with a human telomerase catalytic protein subunit, was kindly provided by Dr. Akihiro Umezawa (National Research Institute for Child Health and Development, Tokyo, Japan) [22].

In vitro co-culture system with BM stromal cells to recreate the BM microenvironment

In this study, we used a culture system devised by a modified cell culture insert of Kawada et al. [23]. First, UBE6T-7 stromal cells were cultured with DMEM medium supplemented with 10 % FCS on the reverse side of the polyethylene terephthalate track-etched membrane of a cell culture insert (35-3495, high pore density cell culture insert; Becton–Dickinson, San Jose, CA, USA) in a 24-well plate (35-3504; Becton–Dickinson). After obtaining a confluent feeder layer, the medium was changed to RMPI1640 medium supplemented with 10 % FCS. MM cells were seeded on the upper side of the membrane of the insert where cytoplasmic villi of UBE6T-7 cells passed through the etched 0.4-μm pores. In this system, even though they directly adhered to UBE6T-7 cells during culture, co-cultured MM cells could easily be harvested without contamination by UBE6T-7 cells. In another condition, UBE6T-7 cells were cultured at the bottom of wells in a 24-well plate (35-3504; Becton–Dickinson). After obtaining a confluent feeder layer, the medium was changed to RMPI1640 medium supplemented with 10 % FCS. MM cells were seeded on the upper side of the insert (35-3095, low pore density cell culture insert; Becton–Dickinson). Under this condition, MM cells were physically separated from the stromal layer, providing an adhesion-negative control.

MTT cell proliferation assays

Cell proliferation was monitored using a Cell Counting Kit (Wako Biochemicals). In brief, cells were seeded in 96-well flat-bottomed microplates at a density of 1×10^5 cells per well and incubated with or without drugs for 72 h at 37 °C. After incubation, the absorbance of reduced MTT was measured at a wavelength of 450 nm using a microplate reader and expressed as a percentage of the value of corresponding untreated cells [24].

The isobologram of Steel and Peckham

We evaluated cytotoxic interactions of bortezomib and other agents at the point of IC_{80} using the isobologram of Steel and Peckham [25]. The IC_{80} was defined as the concentration of drug that produced 80 % cell growth

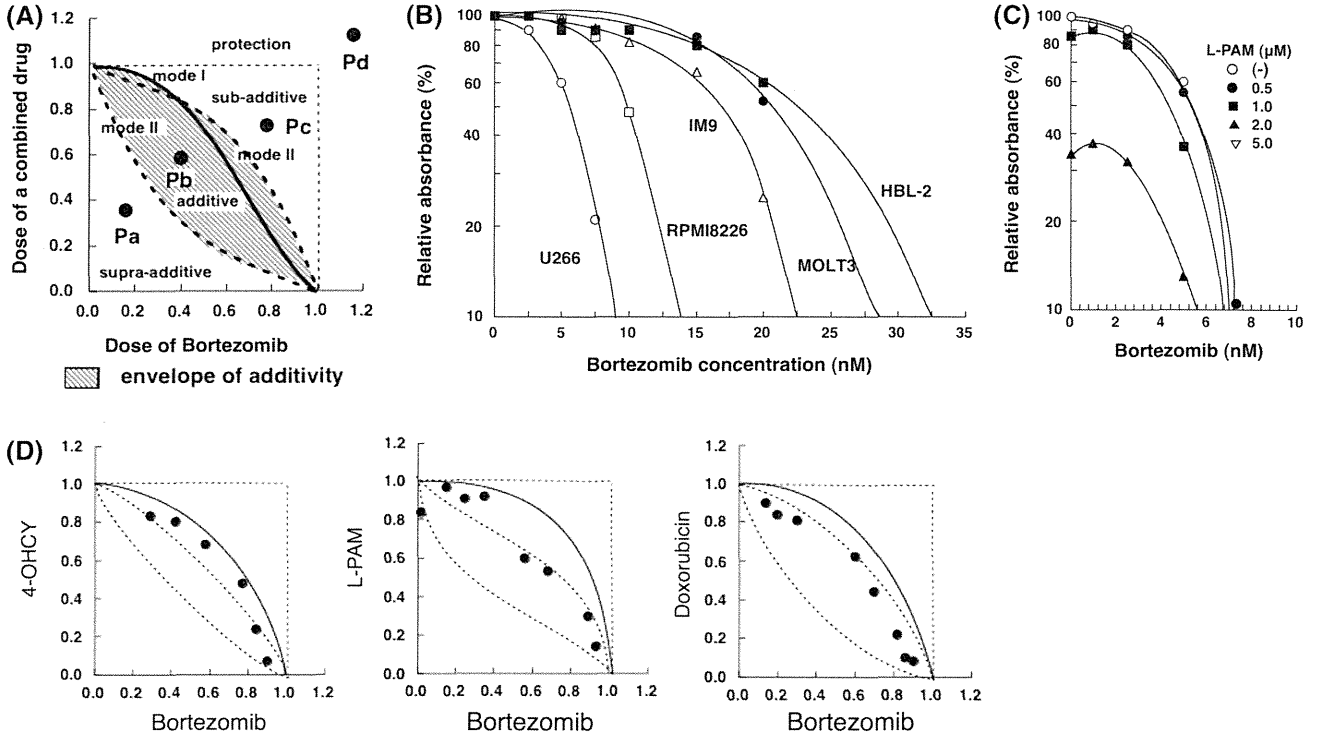

Fig. 1 Cytotoxic interactions of bortezomib and other anti-myeloma agents analyzed by the isobologram of Steel and Peckham. **a** Schematic representation of an isobologram of Steel and Peckham. The concentrations that produced 80 % cell growth inhibition are expressed as 1.0 on the ordinate and the abscissa of isobolograms. The envelope of additivity, surrounded by mode I (*solid line*) and mode II (*broken lines*) isobologram lines, is constructed from the dose–response curves of bortezomib and a combined drug. When the data points of the drug combination fall within the envelope of additivity (Pb), the combination is regarded as additive. When the data points fall to the *left* of the envelope (Pa), the drug combination is regarded as supra-additive (synergism). When the points fall to the *right* of the envelope but within the *square* or on the *square line* (Pc), the combination is regarded as sub-additive. When the data points are *outside* the *square* (Pd), the combination is regarded as protective (antagonism). **b** We cultured U266, RPMI8226, IM9, MOLT3 and HBL-2 cells with various concentrations of bortezomib for 72 h. Cell proliferation was measured by MTT assays. Absorbance at 450 nm is shown on the *y*-axis as a percentage of the values of corresponding untreated cells. *Each point* represents the mean value of at least 10 independent experiments; the SEMs were less than 25 % and were omitted. **c** U266 cells were cultured with various concentrations of bortezomib and melphalan (L-PAM) for 72 h. Cell growth was measured by MTT assays and plotted as a percentage of the value of untreated cells. The concentrations of bortezomib and melphalan (L-PAM) are indicated on the abscissa and the *right upper part* of the *panel*. *Each point* represents the mean value of at least three independent experiments; the SEMs were less than 20 % and were omitted. **d** Isobolograms of bortezomib in combination with 4-OHCY, melphalan (L-PAM) or doxorubicin in U266 cells are shown. *Each point* represents the mean value of at least three independent experiments; the SEMs were less than 25 % and were omitted

inhibition; that is 80 % reduction of absorbance. We have previously described the theoretical basis of the method and the procedure for making isobolograms in detail [26, 27]. In brief, three isoeffect curves were constructed based upon the dose–response curves of bortezomib and other agents (Fig. 1a). If two agents act additively by independent mechanisms, combined data points lie near the Mode I line (hetero-addition). If two agents act additively by similar mechanisms, combined data points lie near the Mode II lines (iso-addition). Because we cannot determine in advance whether the combined effects of two agents would be hetero-additive, iso-additive, or have an intermediate effect between these extremes, all possibilities should be considered. Thus, when the data points of the drug combination fall within the area surrounded by three lines (envelope of additivity), the combination is regarded as additive. The envelope of additivity should not be considered as a reliable definition of additivity. The expression of uncertainty is an important concept of the isobologram method of Steel and Peckham. When the data points fall to the left of the envelope, i.e., the combined effect is caused by lower doses of the two agents than was predicted, we regard the drug combination as supra-additive/synergistic. When the points fall to the right of the envelope, i.e., the combined effect is caused by higher doses of the two agents than was predicted, but within the square or on the line of the square, we regard the combination as sub-additive, i.e., the combination is superior or equal to a single agent but is less than additive. When the data points are outside the square, the combination is

regarded as protective, i.e., the combination is inferior to a single agent in cytotoxic action. Both sub-additive and protective interactions are regarded as antagonism.

The isobologram of Chou and Talalay

Th cytotoxic interaction was also evaluated using the method of Chou and Talalay [28, 29]. We generated isobolograms and calculated the combination index (CI) of bortezomib and other drugs using CompuSyn software according to the manufacturer's instructions (http://www.combosyn.com).

Data analysis

To determine whether the condition of synergism (or antagonism) truly existed, we performed the Wilcoxon signed-rank test to compare the observed data with the predicted minimum (or maximum) data as described previously [26, 27]. Probability values $P < 0.05$ were considered significant. Combinations with $P > 0.05$ were regarded as having an additive/synergistic or additive/antagonistic effect. We used the Stat View 4.01 software program (Abacus Concepts, Berkeley, CA, USA) for statistical analysis.

Immunoblotting

Immunoblotting was carried out according to the standard method using specific antibodies against caspase-3, CHOP and GAPDH (Cell Signaling Technology, Beverly, MA, USA) [30].

Results

Higher sensitivity of MM cell lines to bortezomib than non-MM cell lines

First, we determined the sensitivity of five cell lines, including two MM cell lines, to bortezomib. The dose–response curves of bortezomib for U266, RPMI8226, IM9, MOLT3 and HBL-2 are shown in Fig. 1b. Among these cell lines, the growth of MM cell lines was inhibited at lower concentrations than non-MM cell lines, reproducing the higher sensitivity of MM cells to bortezomib in vitro. The IC_{80} values of bortezomib were calculated based on the dose–response curves: 5.4 ± 0.7 nM for U266, 9.8 ± 1.1 nM for RPMI8226, 16.7 ± 2.2 nM for IM9, 21.2 ± 3.5 nM for MOLT3 and 22.7 ± 3.8 nM for HBL-2. We also determined the IC_{80} levels of other drugs used in the present study for MM cell lines for combination studies (data not shown).

Cytotoxic interactions between bortezomib and other anti-myeloma drugs in liquid culture

We analyzed the cytotoxic interactions between bortezomib and other drugs using the isobologram method of Steel and Peckham as described in the "Materials and methods" section. To generate isobolograms, we first obtained the dose–response curves of bortezomib in combination with other drugs. As an example, Fig. 1c shows the dose–response curves of bortezomib in combination with melphalan in U266 cells. Based on the dose–response curves, we generated the isobologram to analyze the combined effects of bortezomib and melphalan, in which data points of the combination are distributed in the area of supra-additivity to sub-additivity, but mostly in the area of additivity (Fig. 1d, middle panel). This indicates that the combination of bortezomib and melphalan exerts an additive or synergistic cytotoxicity in U266 cells. In contrast, all but two data points fell in the area of sub-additivity in isobolograms of bortezomib in combination with 4-OHCY, suggesting that this combination is not so favorable (Fig. 1d, left panel). In the bortezomib and doxorubicin combination, all data points fell in the area of additivity, indicating that the two drugs are additive in U266 cells (Fig. 1d, right panel). The difference among melphalan, 4-OHCY and doxorubicin was statistically significant: the mean values of observed data were 0.55 (predicted range: 0.57–0.83; $P < 0.05$ by the Wilcoxon signed-rank test), 0.62 (predicted range: 0.42–0.77; $P > 0.05$) and 0.54 (predicted range: 0.38–0.82; $P > 0.05$) for melphalan, 4-OHCY and doxorubicin, respectively, in combination with bortezomib (Table 1). The virtually identical results were obtained in RPMI8226 cells (Table 1). Furthermore, the combination of bortezomib and dexamethasone yielded synergistic cytotoxicity in both U266 and RPMI8226 cell lines (Table 1), providing a rationale for the inclusion of corticosteroids in bortezomib-based regimens for MM. Because these preliminary data were obtained in adhesion-free liquid culture, we attempted to confirm the results under conditions closer to in vivo in the following step.

Establishment of the in vitro culture systems to recreate the BM microenvironment

It is well conceived that MM cells expand in the BM microenvironment and acquire drug resistance through the interaction with stromal cells and extracellular matrix proteins [19, 20]. We therefore established in vitro culture systems recapitulating the BM microenvironment to investigate cytotoxic interactions of bortezomib and other anti-cancer drugs against MM cells under conditions closer to in vivo. To this end, we first used fibronectin-coated plates, because the adhesion-mediated signals between

Table 1 Quantitative analysis of the combination of bortezomib and other drugs in myeloma cells

Combined drugs	Cell lines	Data points	Observed data*	Predicted min.**	Predicted max.***	Effects#
Melphalan	U266	8	0.55	0.57	0.83	Synergistic
	RPMI8226	8	0.40	0.50	0.77	Synergistic/additive
4-OHCY	U266	6	0.62	0.42	0.77	Additive
	RPMI8226	6	0.65	0.62	0.75	Additive
Doxorubicin	U266	8	0.54	0.38	0.82	Additive
	RPMI8226	6	0.66	0.37	0.79	Additive
Dexamethasone	U266	6	0.87	0.63	0.99	Synergistic
	RPMI8226	8	0.54	0.61	0.80	Synergistic

* Mean values of observed data (SD not shown)

** Mean values of the predicted minimum values for an additive effect (SD not shown)

*** Mean values of the predicted maximum values for an additive effect (SD not shown)

Overall effect of drug combination was evaluated by the Wilcoxon signed-rank test. If the observed values are significantly ($P < 0.05$) smaller than the predicted minimum values, the combination is regarded as synergistic. If P values are >0.05, the combination is regarded as additive/synergistic. If the observed data fall between the predicted minimum and maximum values, the combination is regarded as additive

fibronectin and VLA-4 play critical roles in the establishment of CAM-DR in MM cells [12, 13]. We treated KMS12-BM and RPMI8226 cells with either 4-OHCY or doxorubicin in microplates coated with or without fibronectin. As anticipated, the presence of fibronectin significantly attenuated the cytotoxic activity of 4-OHCY (Fig. 2a) and doxorubicin (Fig. 2b) in both cell lines, recapitulating the fibronectin-mediated drug resistance in vitro.

Second, we constructed a co-culture system using a cell culture insert, which allows co-culture of MM and stromal cells with or without direct contact (Fig. 2c). Using this system, we treated MM cell lines with either 4-OHCY or doxorubicin with or without direct adhesion to stromal cells. As shown in Fig. 2d, direct contact with stromal cells significantly reduced the cytotoxic activity of 4-OHCY and doxorubicin in KMS12-BM cells. The virtually identical results were obtained in RPMI8226 cells (data not shown). These results validate that the direct adhesion to stromal cells confers strong drug resistance to MM cells, reproducing CAM-DR in vitro. Using this system, we investigated the combined effects of bortezomib with other anticancer drugs under the conditions resembling the BM microenvironment in vivo.

Cytotoxic interactions between bortezomib and other anti-myeloma drugs in contact with fibronectin or stromal cells

Recently, bortezomib-based regimens, such as VMP, VCD, PAD and RVd, have been used for the initial treatment of MM with considerable success [14–18]. These regimens are composed of bortezomib, corticosteroids and one additional drug; melphalan, cyclophosphamide, doxorubicin or lenalidomide. It is important to determine which drug makes the most effective combination with bortezomib in preclinical studies, because it is not realistic to accomplish this with clinical trials. We, therefore compared the combined effects of the four drugs with bortezomib under stroma-free conditions and in contact with fibronectin or stromal cells using the isobologram of Chou and Talalay instead of the isobologram of Steel and Peckham, because the former allows quantitative assessment of the combined effects more easily and objectively [28].

To generate isobolograms, we first obtained the dose–response curves of bortezomib in combination with the four drugs under each culture condition (data not shown). Then, we generated non-constant normalized isobolograms and determined the CI values at IC_{50} using CompuSyn software [28, 29]. Figure 3a shows the definition of the combined effects according to the location of data points in the isobologram generated by this method. Figure 3b shows representative isobolograms of the combined effects of bortezomib and the four drugs in RPMI8226 cells under stroma-free conditions. The results of the same analyses performed in contact with fibronectin and stromal cells are shown in Fig. 3c and d, respectively. It is of note that all data points of the combination with melphalan fell within the area of synergism or additivity under stroma-free conditions and within the area of additivity even in the presence of fibronectin or stromal cells. Most of the data points of the doxorubicin combination fell in the area of additivity, whereas those of 4-OHCY were mostly in the area of antagonism under any conditions. These results suggest that melphalan and doxorubicin make favorable combinations with bortezomib, but 4-OHCY is rather

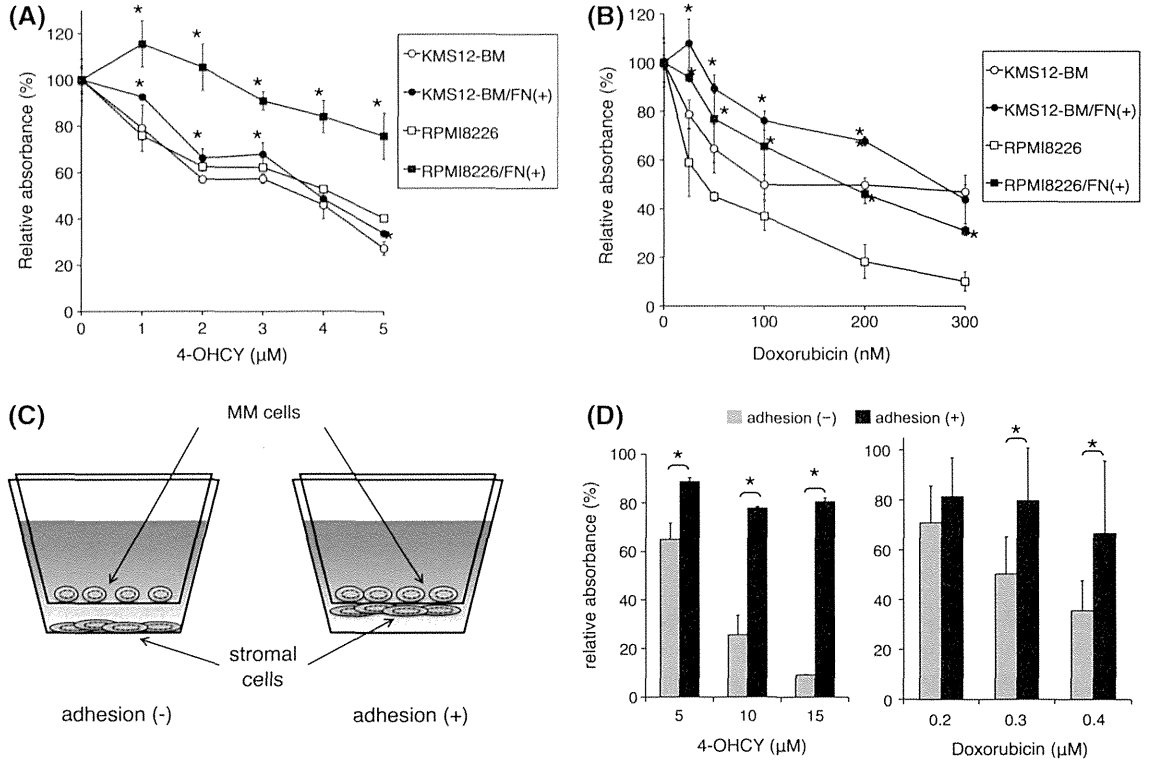

Fig. 2 Establishment of in vitro culture systems for recreating the bone marrow microenvironment. **a** KMS12-BM and RPMI8226 cells were cultured with various concentrations of 4-OHCY in 96-well plates coated with (*filled circle/square*) or without (*open circle/square*) fibronectin (FN) for 72 h. Cell proliferation was measured by MTT assays and expressed as a percentage of the values of corresponding untreated cells. **b** The same experiment was performed with doxorubicin. The mean ± SD (*bars*) of three independent experiments are shown. *P* values were calculated by one-way ANOVA with the Student–Newman–Keuls multiple comparisons test. $^*P < 0.05$. **c** Diagram of the culture system used in this study. See "Materials and methods" for detailed description of the culture. **d** KMS12-BM cells were cultured in the absence or presence of either 4-OHCY (*left*) or doxorubicin (*right*) in a cell culture insert with or without direct adhesion to UBE6T-7 stromal cells. After 72 h culture, cells were harvested and subjected to MTT assays for cell proliferation, which is expressed as a percentage of the values of corresponding untreated cells. The mean ± SD (*bars*) of three independent experiments are shown. *P* values were calculated by one-way ANOVA with the Student–Newman–Keuls multiple comparisons test. $^*P < 0.05$

antagonistic, regardless of the culture conditions of RPMI8226 cells.

Next, we quantitatively compared the CI values of bortezomib in combination with the four drugs in KMS12-BM and RPMI8226 cells under three culture conditions. The CI values of bortezomib and melphalan were mostly lower than those of other combinations in both cell lines not only under stroma-free conditions (Fig. 4a), but also in contact with fibronectin (Fig. 4b) or stromal cells (Fig. 4c). These results suggest that melphalan has stronger combined effects with bortezomib on MM cells than other agents under any circumstances. In contrast, cyclophosphamide was mostly sub-additive with bortezomib and antagonistic in the presence of stromal cells. Doxorubicin showed additive effects under stroma-free conditions and in contact with fibronectin, but was rather antagonistic when stromal cells were present (Fig. 4c). Consistent with these results, melphalan enhanced bortezomib-induced caspase-3 activation significantly stronger than 4-OHCY and doxorubicin did at equitoxic concentrations in RPMI8226 cells in contact with stromal cells (Fig. 5a, b).

On the other hand, CI values of lenalidomide in combination with bortezomib were equal to or even higher than those of melphalan and doxorubicin under stroma-free conditions (Fig. 4a) and in contact with fibronectin (Fig. 4b). However, CI values were equal to or even lower than those of other agents in the presence of stromal cells (Fig. 4c). In support of this observation, the combination of bortezomib and lenalidomide readily increased the expression of CCAAT/enhancer-binding protein homologous protein (CHOP), a pro-apoptotic transcription factor induced by excessive protein overload in the endoplasmic reticulum (ER) and subsequent activation of ATF4 [31, 32], in RPMI8226 cells in the presence of stromal cells (Fig. 5c, d). This suggests that the cytotoxic action of the two drugs converges at the unfolded protein response, leading to ER stress-induced apoptosis.

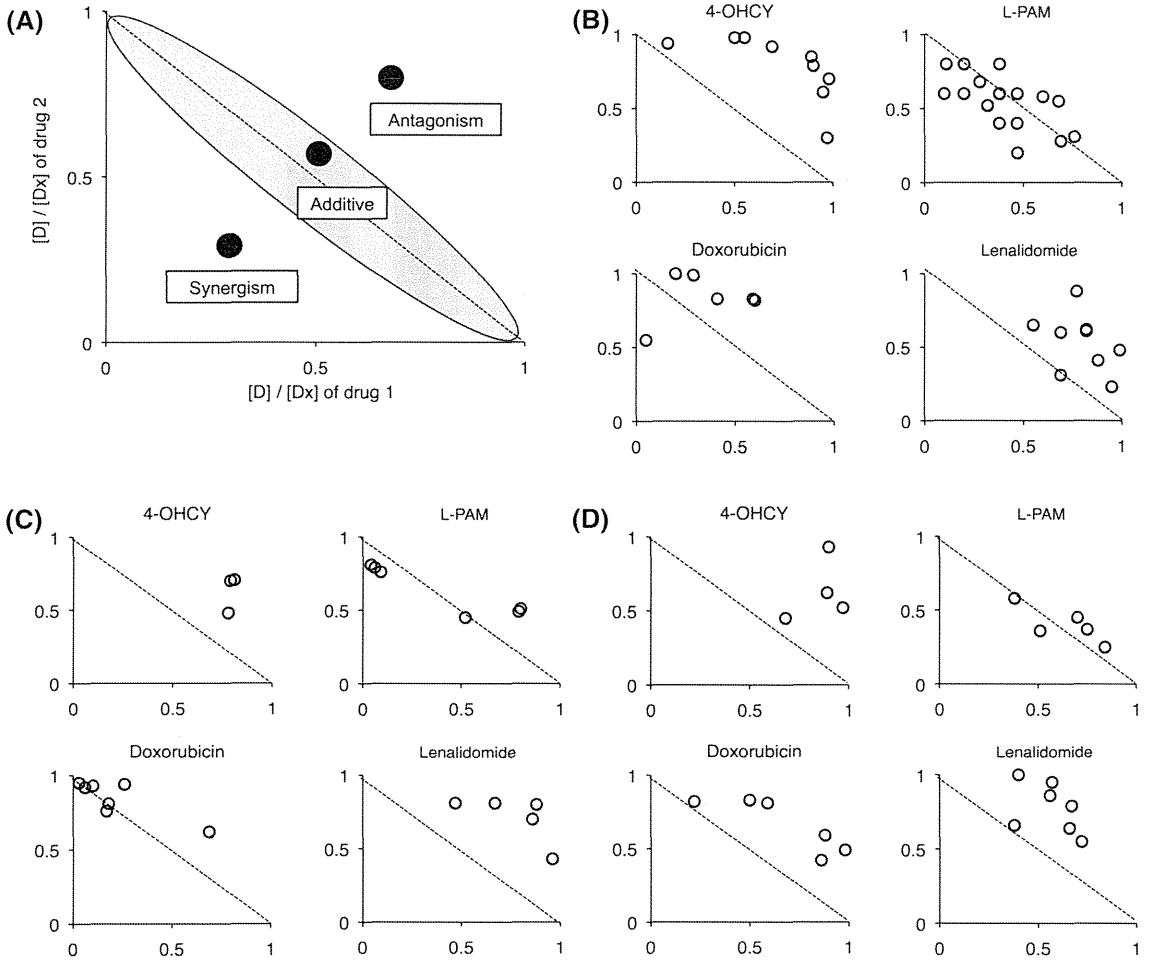

Fig. 3 Isobologram analysis of cytotoxic interaction of bortezomib and other anti-myeloma agents under stroma-free conditions and in contact with fibronectin or stromal cells. **a** Schematic representation of the non-constant normalized isobologram of Chou and Talalay. When the data points of the drug combination fall within the *shaded area* (envelope), the combination is regarded as additive. When the data points fall to the *left* and *right* of the envelope, the drug combination is regarded as synergistic and antagonistic, respectively. **b** RPMI8226 cells were treated with bortezomib in combination with the indicated drugs under stroma-free conditions for 72 h. **c** RPMI8226 cells were treated with bortezomib in combination with the indicated drugs in contact with fibronectin for 72 h. **d** RPMI8226 cells were treated with bortezomib in combination with the indicated drugs in contact with stromal cells for 72 h. Cell proliferation was measured by MTT assays and expressed as a percentage of that of the corresponding untreated cells. Dose–response curves of each combination were generated to make non-constant normalized isobolograms. The isobolograms shown are representative of at least three independent experiments. *Each point* represents the mean value of at least three independent experiments; the SEMs were less than 25 % and were omitted

Discussion

In this study, we investigated the cytotoxic interaction of bortezomib with four anti-myeloma drugs (melphalan, cyclophosphamide, doxorubicin and lenalidomide) under stroma-free conditions and in contact with fibronectin or bone marrow stromal cells using isobologram methods. We found that, among the four key anti-myeloma drugs, melphalan makes the best combination with bortezomib under any conditions, and thus, is considered the most suitable drug to be combined with bortezomib for MM treatment along with corticosteroids, which also exert a strong synergistic effect with bortezomib. This finding is consistent with clinical evidence that the combination of bortezomib, melphalan and prednisone (VMP) has an obvious survival benefit demonstrated in phase III trials as a frontline therapy for transplantation-ineligible MM patients, and thus, is recommended as a Grade A/Category 1 regimen in the guidelines of the International Myeloma Working Group, National Comprehensive Cancer Network, Japanese Society of Myeloma, and Japanese Society of Hematology [33, 34]. Unexpectedly, 4-OHCY, an active metabolite of cyclophosphamide, was antagonistic with bortezomib especially in the presence of stromal cells. In

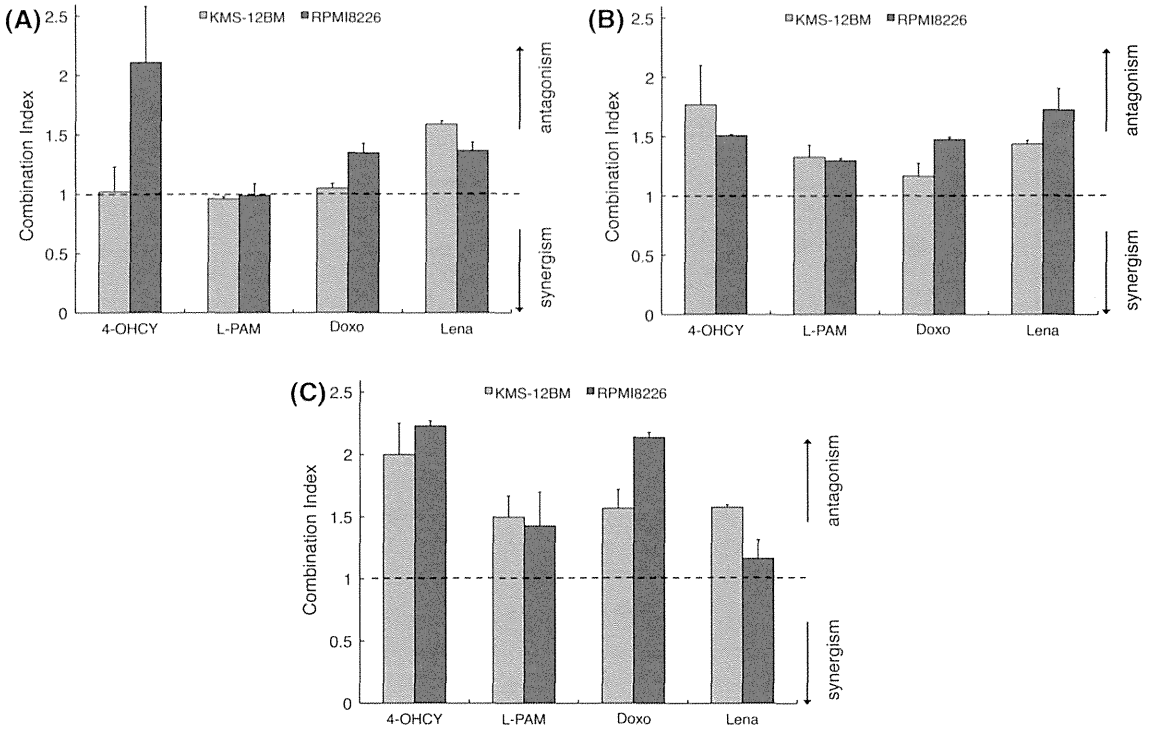

Fig. 4 CI values of the combination of bortezomib and other anti-myeloma agents determined by isobolograms of Chou and Talalay. The combination index (CI) was calculated by the method of Chou and Talalay, based on the dose–response curves of bortezomib in combination with the indicated agents in KMS-12BM and RPMI8226 cells. CI values under stroma-free conditions (**a**), in contact with fibronectin (**b**), and in contact with stromal cells (**c**) are shown. Data are the mean ± SD (*bars*) of three independent experiments

fact, the combination of bortezomib, cyclophosphamide and dexamethasone is not recommended for transplantation-eligible, -ineligible or relapsed/refractory cases in any guidelines because of the lack of concrete clinical evidence to support the use of this combination as a first-line treatment at present, although it is possible that the CyBorD combination will be included in the Grade A/Category 1 regimens for pre-transplantation settings in the future [35].

Myeloma cells may mimic plasma cell leukemia under stroma-free culture conditions and provide a clue to develop better treatment strategies for this highly intractable disease [36]. Moreover, RPMI8226 and U266 cell lines are suitable for this purpose because they were established from peripheral blood of myeloma patients [21]. The present study revealed that melphalan and doxorubicin made better combination with bortezomib than 4-OHCY and lenalidomide in RPMI8226 and U266 cells under stroma-free conditions. This is consistent with recent clinical findings that treatment outcome of plasma cell leukemia has been significantly improved by bortezomib in combination with either melphalan or doxorubicin with or without stem cell support [37–39].

Currently, it is unclear why the two SN2 alkylating agents with similar mechanisms of action exert contrasting effects in combination with bortezomib even in the absence of cell adhesion. This might be explained by the different kinetics of DNA damage induction between the two drugs. The formation of interstrand DNA crosslinks peaks at 4–8 and 16 h of treatment with cyclophosphamide and melphalan, respectively [40, 41]. Furthermore, cyclophosphamide-induced DNA crosslinks are almost completely repaired within 24 h by the Fanconi pathway [40], whereas those by melphalan last longer, with approximately 40 % of the lesions remaining after 40 h of treatment [41]. Bortezomib blocks the repair of DNA interstrand crosslinks at the initial step via interruption with the activation of the Fanconi pathway [42–44]. Therefore, it is likely that bortezomib interferes with the repair process of melphalan-induced DNA damage more profoundly than that of cyclophosphamide-induced damage because of the long-lasting nature of the former, thereby causing more favorable combined effects with melphalan. This argument raises another important matter of debate: whether the order of addition affects the combined effects of bortezomib and other agents, especially melphalan.

The major obstacle of the present study is that the combined effect was assessed only with simultaneous addition of two drugs, because washing out the first drug is technically impossible in the co-culture system using a cell culture insert. This partly explains the discordance between

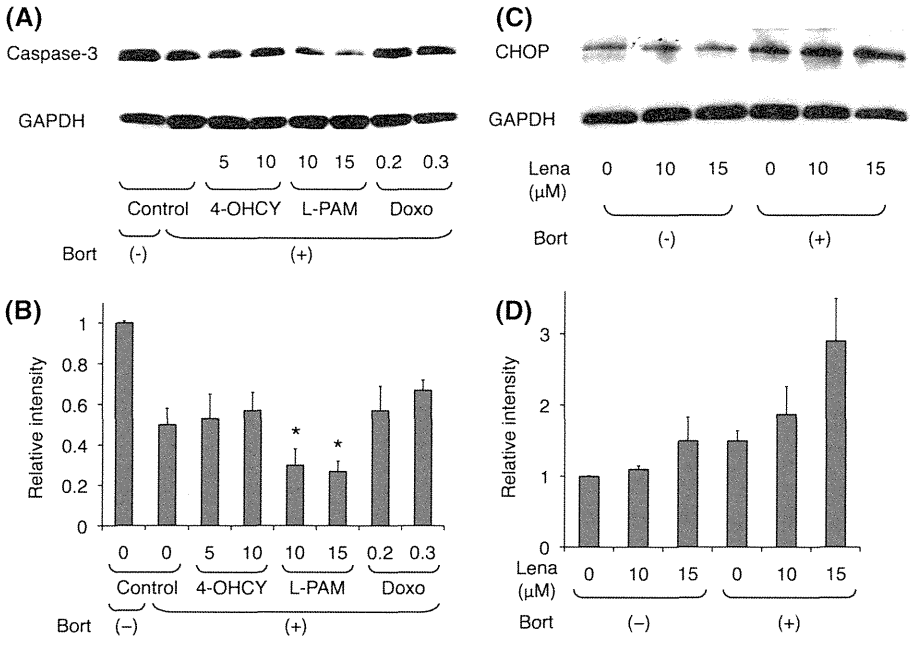

Fig. 5 Effects of bortezomib combinations on the expression of caspase-3 and CHOP in RPMI8226 cells. **a** RPMI8226 cells were cultured in the absence (−) or presence (+) of 5 nM bortezomib in combination with IC_{20} and IC_{50} doses of 4-OHCY, melphalan (L-PAM) and doxorubicin (Doxo). After 48 h, whole cell lysates were prepared and subjected to immunoblotting for the expression of full-length caspase-3 and GAPDH (internal control). **b** The signal intensities of each band in (**a**) were quantified, normalized to those of the corresponding GAPDH, and shown as relative values of caspase-3 expression setting the untreated control to 1.0. *P* values were calculated by one-way ANOVA with the Student–Newman–Keuls multiple comparisons test. $^*P < 0.05$ against other bortezomib combinations. **c** RPMI8226 cells were cultured in the absence (−) or presence (+) of 5 nM bortezomib in combination with IC_{20} and IC_{50} doses of lenalidomide (Lena). After 48 h, whole cell lysates were prepared and subjected to immunoblotting for the expression of CHOP and GAPDH (internal control). **d** The signal intensities of each band in (**c**) were quantified, normalized to those of the corresponding GAPDH, and shown as relative values of CHOP expression setting the untreated control to 1.0

the present data and clinical observations that cyclophosphamide and doxorubicin are highly effective in bortezomib-based triplet regimens [15, 18, 35]. Sequential additions may yield different results and provide further information for clinical translation. A few studies have been published addressing this issue under adhesion-free conditions. Mitsiades et al. [45] reported that the synergistic effect of bortezomib and doxorubicin was significantly enhanced when myeloma cells were treated with doxorubicin first, followed by bortezomib. They speculated that bortezomib inhibits the repair of doxorubicin-induced DNA damage by down-regulating the expression of repair factors such as DNA-dependent protein kinase, Ku80 and topoisomerase IIβ. As bortezomib also represses the expression of 8-Oxoguanine DNA glycosylase and uracil-DNA glycosylase, which play a critical role in the repair of alkylated DNA [46], this scenario may be applicable to the combination of bortezomib and alkylating agents. Indeed, the schedule-dependent effect of bortezomib and melphalan has been reported by Popat et al. [47], showing that synergistic cytotoxicity was observed only in melphalan pre-exposure but not other schedules (bortezomib pre-exposure and simultaneous addition) in co-culture experiments. In a phase I/II trial combining high-dose melphalan and autologous transplant with bortezomib for MM, Lonial et al. [48] demonstrated that the levels of apoptosis in bone marrow myeloma cells were significantly higher in patients who received bortezomib 24 h after high-dose melphalan conditioning than in those who received bortezomib 24 h before melphalan. A similar phenomenon was observed in the combination of bortezomib and anti-metabolites in other malignancies: the combined effects were robustly enhanced when bortezomib was added after gemcitabine in pancreas cancer cells [49] or cytosine arabinoside in mantle cell lymphoma cells [50]. These findings may provide important information for designing effective clinical protocols for myeloma and other intractable malignancies.

Finally, the favorable combined effect of bortezomib and lenalidomide in the presence of stromal cells is an important finding and deserves further investigation. Lenalidomide may act on stromal cells to disrupt stroma-derived anti-apoptotic signals to MM cells via interference with the function and expression of surface molecules on stromal cells [51, 52]. Bortezomib also has the ability to overcome CAM-DR by down-regulating the expression of

VLA-4 [8, 9]. As such, physical and functional disruption of stroma–myeloma cell interactions may underlie the synergistic effect of the two drugs. In addition, thalidomide and its derivatives, including lenalidomide, were reported to bind to cereblon, a component of E3 ubiquitin ligase complex, and perturb ubiquitination and the subsequent degradation of multiple cellular proteins [53, 54]. Therefore, the cytotoxic action of bortezomib and lenalidomide converges at the unfolded protein response, leading to excessive protein overload and the resultant ER stress-induced apoptosis [31, 32]. It is reasonable to speculate that this lethal communication underlies the synergism of bortezomib and lenalidomide, as evidenced by a marked increase in CHOP expression in RPMI8226 cells treated with bortezomib and lenalidomide in this study.

In conclusion, although there are a number of difficulties in the translation of the results of in vitro studies to the bedside, our findings may be of help for the selection of bortezomib-based regimens for patients with multiple myeloma as well as plasma cell leukemia.

Acknowledgments The authors are grateful to Drs. Yasuhiko Kano (Tochigi Cancer Center) and Kaoru Noborio-Hatano (Jichi Medical School) for their technical advice regarding the generation of the isobologram of Steel and Peckham, Professor Kiyoshi Ando (Tokai University) for technical advice regarding the establishment of the co-culture system, and Ms. Akiko Yonekura for technical assistance. This work was supported in part by the High-Tech Research Center Project for Private Universities: Matching Fund Subsidy from MEXT, a Grant-in-Aid for Scientific Research from JSPS, and research grants from Japan Leukemia Research Fund, Osaka Cancer Foundation (to YF and JK), Takeda Science Foundation, Kano Foundation and Mitsui Life Social Welfare Foundation (to JK). YF is a winner of the Award in Aki's Memory from the International Myeloma Foundation Japan.

Conflict of interest YF received research funding and honoraria from Janssen Pharmaceutical K.K. The other authors have no conflicts of interest.

References

1. Moreau P, Richardson PG, Cavo M, Orlowski RZ, San Miguel JF, Palumbo A, Harousseau JL. Proteasome inhibitors in multiple myeloma: 10 years later. Blood. 2012;120:947–59.
2. Suzuki K. Current therapeutic strategy for multiple myeloma. Jpn J Clin Oncol. 2013;43:116–24.
3. Weissman AM, Shabek N, Ciechanover A. The predator becomes the prey: regulating the ubiquitin system by ubiquitination and degradation. Nat Rev Mol Cell Biol. 2011;12:605–20.
4. Frankland-Searby S, Bhaumik SR. The 26S proteasome complex: an attractive target for cancer therapy. Biochem Biophys Acta. 2012;1825:64–76.
5. Fotheringham S, Epping MT, Stimson L, Khan O, Wood V, Oezzella F, et al. Genome-wide loss-of-function screen reveals an important role for the proteasome in HDAC inhibitor-induced apoptosis. Cancer Cell. 2009;15:57–66.
6. Kikuchi J, Wada T, Shimizu R, Izumi T, Akutsu M, Mitsunaga K, et al. Histone deacetylases are critical targets of bortezomib-induced cytotoxicity in multiple myeloma. Blood. 2010;116:406–17.
7. Mannava S, Zhuang D, Nair JR, Bansal R, Wawrzyniak JK, Zucker SN, et al. KLF9 is a novel transcriptional regulator of bortezomib- and LBH589-induced apoptosis in multiple myeloma cells. Blood. 2012;119:1450–8.
8. Yanamandra N, Colaco NM, Parquet NA, Buzzeo RW, Boulware D, Wright G, et al. Tipifarnib and bortezomib are synergistic and overcome cell adhesion-mediated drug resistance in multiple myeloma and acute myeloid leukemia. Clin Cancer Res. 2006;12:591–9.
9. Noborio-Hatano K, Kikuchi J, Takatoku M, Shimizu R, Wada T, Ueda M, et al. Bortezomib overcomes cell-adhesion-mediated drug resistance through downregulation of VLA-4 expression in multiple myeloma. Oncogene. 2009;28:231–42.
10. Srypayap P, Nagai T, Hatano K, Kikuchi J, Furukawa Y, Ozawa K. Romidepsin overcomes cell adhesion-mediated drug resistance in multiple myeloma cells. Acta Haematol. 2014;132:1–4.
11. Zhang B, Strauss AC, Chu S, Li M, Ho Y, Shiang K-D, et al. Effective targeting of quiescent chronic myelogenous leukemia stem cells by histone deacetylase inhibitors in combination with imatinib mesylate. Cancer Cell. 2010;17:427–42.
12. Nefedova Y, Landowski TH, Dalton WS. Bone marrow stromal-derived soluble factors and direct cell contact contribute to de novo drug resistance of myeloma cells by distinct mechanisms. Leukemia. 2003;17:1175–82.
13. Podar K, Zimmerhackl A, Fulciniti M, Tonon G, Hainz U, Tai Y-T, et al. The selective adhesion molecule inhibitor Natalizmab decreases multiple myeloma cell growth in the bone marrow microenvironment: therapeutic implications. Br J Haematol. 2011;155:438–48.
14. Miguel JS, Shlag R, Khuageva NK, Dimopoulos MA, Shpilberg O, Kropff M, et al. Persistent overall survival benefit and no increased risk of second malignancies with bortezomib-melphalan-prednisone versus melphalan-prednisone in patients with previously untreated multiple myeloma. J Clin Oncol. 2013;31:448–55.
15. Kumar S, Finn I, Richardson PG, Hari P, Callander N, Noga SJ, et al. Randomized, multicenter, phase 2 study (EVOLUTION) of combinations of bortezomib, dexamethasone, cyclophosphamide, and lenalidomide in previously untreated multiple myeloma. Blood. 2012;119:4375–82.
16. Ludwig H, Viterbo L, Greil R, Masszi T, Spicka I, Shpilberg O, et al. Randomized phase II study of bortezomib, thalidomide, and dexamethasone with or without cyclophosphamide as induction therapy in previously untreated multiple myeloma. J Clin Oncol. 2013;31:247–55.
17. Richardson PG, Weller E, Lonial S, Jakubowiak AJ, Jagannath S, Raje NS, et al. Lenalidomide, bortezomib, and dexamethasone combination therapy in patients with newly diagnosed multiple myeloma. Blood. 2010;116:679–86.
18. Takamatsu Y, Sunami K, Muta T, Morimoto H, Miyamoto T, Higuchi M, et al. Bortezomib, doxorubicin and intermediate-dose dexamethasone (iPAD) therapy for relapsed or refractory multiple myeloma: a multicenter phase 2 study. Int J Hematol. 2013;98:179–85.
19. Hideshima T, Mitsiades C, Tonon G, Richardson PG, Anderson KC. Understanding multiple myeloma pathogenesis in the bone marrow to identify new therapeutic targets. Nat Rev Cancer. 2007;7:585–98.
20. Abe M. Targeting the interplay between myeloma cells and the bone marrow microenvironment in myeloma. Int J Hematol. 2011;94:334–43.
21. Drexler HG, Matsuo Y, MacLeod RA. Persistent use of false myeloma cell lines. Hum Cell. 2003;16:101–5.
22. Mori T, Kiyono T, Imabayashi H, Takeda Y, Tsuchiya K, Miyoshi S, et al. Combination of hTERT and bmi-1, E6, or E7

induces prolongation of the life span of bone marrow stromal cells from an elderly donor without affecting their neurogenic potential. Mol Cell Biol. 2005;25:5183–95.
23. Kawada H, Ando K, Tsuji T, Shimaoka Y, Nakamura Y, Chargui J, et al. Rapid ex vivo expansion of human umbilical cord blood hematopoietic progenitors using a novel culture system. Exp Hematol. 1999;27:904–15.
24. Shimizu R, Kikuchi J, Wada T, Ozawa K, Kano Y, Furukawa Y. HDAC inhibitors augment cytotoxic activity of rituximab by up-regulating CD20 expression on lymphoma cells. Leukemia. 2010;24:1760–8.
25. Steel GG, Peckham MJ. Exploitable mechanisms in combined radiotherapy-chemotherapy: the concept of additivity. Int J Radiat Oncol Biol Phys. 1979;5:85–93.
26. Kano Y, Akutsu M, Tsunoda S, Mano H, Sato Y, Honma Y, et al. In vitro cytotoxic effects of a tyrosine kinase inhibitor STI571 in combination with commonly used antileukemic agents. Blood. 2001;97:1999–2007.
27. Furukawa Y, Vu HA, Akutsu M, Odgerel T, Izumi T, Tsunoda S, et al. Divergent cytotoxic effects of PKC412 in combination with conventional antileukemic agents in FLT3 mutation-positive versus -negative leukemia cell lines. Leukemia. 2007;21:1005–14.
28. Chou TC. Drug combination studies and their synergy quantification using the Chou-Talalay method. Cancer Res. 2010;70:440–6.
29. Kikuchi J, Yamada S, Koyama D, Wada T, Nobuyoshi M, Izumi T, et al. The novel orally active proteasome inhibitor K-7174 exerts anti-myeloma activity in vitro and in vivo by down-regulating the expression of class I histone deacetylases. J Biol Chem. 2013;288:25593–602.
30. Kikuchi J, Shibayama N, Yamada S, Wada T, Nobuyoshi M, Izumi T, et al. Homopiperazine derivatives as a novel class of proteasome inhibitors with a unique mode of proteasome binding. PLoS One. 2013;8:e60649.
31. Ri M, Iida S, Nakashima T, Miyazaki H, Mori F, Ito A, et al. Bortezomib-resistant myeloma cell lines: a role for mutated *PSMB5* in preventing the accumulation of unfolded proteins and fatal ER stress. Leukemia. 2010;24:1506–12.
32. Nakamura S, Miki H, Kido S, Nakano A, Hiasa M, Oda A, et al. Activating transcription factor 4, an ER stress mediator, is required for, but excessive ER stress suppresses osteoblastogenesis by bortezomib. Int J Hematol. 2013;98:66–73.
33. Palumbo A, Sezer O, Kyle R, Miguel JS, Orlowski RZ, Moreau P, et al. International myeloma working group guidelines for the management of multiple myeloma patients ineligible for standard high-dose chemotherapy with autologous stem cell transplantation. Leukemia. 2009;23:1716–30.
34. Watanabe R, Tokuhira M, Kizaki M. Current approaches for the treatment of multiple myeloma. Int J Hematol. 2013;97:333–44.
35. Reeder CB, Reece DE, Kukreti V, Chen C, Trudel S, Hentz J, et al. Cyclophosphamide, bortezomib and dexamethasone induction for newly diagnosed multiple myeloma: high response rates in a phase II clinical trial. Leukemia. 2009;23:1337–41.
36. Fernández de Larrea C, Kyle RA, Durie BGM, Ludwig H, Usmani S, Vesole DH, et al. Plasma cell leukemia: consensus statement on diagnostic requirements, response criteria and treatment recommendations by the International Myeloma Working Group. Leukemia 2013; 27: 780–91.
37. Libby E, Candelaria-Quintana D, Moualla H, Abdul-Jaleel M, Rabinowitz I. Durable complete remission of primary plasma cell leukemia with the bortezomib plus melphalan and prednisone (VMP) regimen. Am J Hematol. 2010;85:733–4.
38. D'Arena G, Valentini CG, Pietrantuono G, Guariglia R, Martorelli MC, Mansueto G, et al. Frontline chemotherapy with bortezomib-containing combinations improves response rate and survival in primary plasma cell leukemia: a retrospective study from GIMEMA Multiple Myeloma Working Party. Ann Oncol. 2012;23:1499–502.
39. Katodritou E, Terpos E, Kelaidi C, Kotsopoulou M, Delimpasi S, Kyrtsonis M-C, et al. Treatment with bortezomib-based regimens improves overall response and predicts for survival in patients with primary or secondary plasma cell leukemia: analysis of the Greek myeloma study group. Am J Hematol. 2014;89:145–50.
40. Johnson LA, Malayappan B, Tretyakova N, Campbell C, MacMillan ML, Wagner JF, Jacobson PA. Formation of cyclophosphamide specific DNA adducts in hematological diseases. Pediatr Blood Cancer. 2012;58:708–14.
41. Spanswick VJ, Craddock C, Sekhar M, Mahendra P, Shankaranarayana P, Hughes RG, et al. Repair of DNA interstrand crosslinks as a mechanism of clinical resistance to melphalan in multiple myeloma. Blood. 2002;100:224–9.
42. Jacquemont C, Taniguchi T. Proteasome function is required for DNA damage response and Fanconi anemia pathway activation. Cancer Res. 2007;67:7395–405.
43. Varde DN, Oliveria V, Mathews L, Wang X, Villagra A, Boulware D, et al. Targeting the Fanconi anemia/BRCA pathway circumvents drug resistance in multiple myeloma. Cancer Res. 2009;69:9367–75.
44. Neri P, Ren L, Gratton K, Stebner E, Johnson J, Klimowicz A, et al. Bortezomib induced "BRCAness" sensitizes multiple myeloma cells to PARP inhibitors. Blood. 2011;118:6368–79.
45. Mitsiades N, Mitsiades CS, Richardson PG, Poulaki V, Tai Y-T, Chauhan D, et al. The proteasome inhibitor PS-341 potentiates sensitivity of multiple myeloma cells to conventional chemotherapeutic agents: therapeutic applications. Blood. 2003;101:2377–80.
46. Fu D, Calvo JA, Samson LD. Balancing repair and tolerance of DNA damage caused by alkylating agents. Nat Rev Cancer. 2012;12:104–20.
47. Popat R, Maharaj L, Oakervee H, Cavenagh J, Joel S. Schedule dependent cytotoxicity of bortezomib and melphalan in multiple myeloma. Br J Haematol. 2013;160:111–4.
48. Lonial S, Kaufman J, Tighiouart M, Nooka A, Langston AA, Heffner LT, et al. A phase I/II trial combining high-dose melphalan and autologous transplant with bortezomib for multiple myeloma: a dose- and schedule-finding study. Clin Cancer Res. 2010;16:5079–86.
49. Fahy BN, Schlieman MG, Virudachalam S, Bold RJ. Schedule-dependent molecular effects of the proteasome inhibitor bortezomib and gemcitabine in pancreatic cancer. J Surg Res. 2003;113:88–95.
50. Weigert O, Pastore A, Rieken M, Lang N, Hiddemann W, Dreyling M. Sequence-dependent synergy of the proteasome inhibitor bortezomib and cytarabine in mantle cell lymphoma. Leukemia. 2007;21:524–8.
51. Quach H, Ritchie D, Stewart AK, Neeson P, Harrison S, Smyth MJ, Prince HM. Mechanism of action of immunomodulatory drugs (IMiDS) in multiple myeloma. Leukemia. 2010;24:22–32.
52. Schortt J, Hsu AK, Johnstone RW. Thalidomide-analogue biology: immunological, molecular and epigenetic targets in cancer therapy. Oncogene. 2013;32:4191–202.
53. Ito T, Ando H, Suzuki T, Ogura T, Hotta K, Imamura Y, et al. Identification of a primary target of thalidomide teratogenicity. Science. 2010;327:1345–50.
54. Lopez-Girona A, Mendy D, Ito T, Miller K, Gandhi AK, Kang J, et al. Cereblon is a direct protein target for immunomodulatory and antiproliferative activities of lenalidomide and pomalidomide. Leukemia. 2012;26:2326–35.

Rapid Communication

Acta Haematologica

Acta Haematol 2014;132:1–4
DOI: 10.1159/000357213

Received: August 8, 2013
Accepted after revision: November 10, 2013
Published online: December 12, 2013

Romidepsin Overcomes Cell Adhesion-Mediated Drug Resistance in Multiple Myeloma Cells

Piyanuch Sripayap[a] Tadashi Nagai[a] Kaoru Hatano[a] Jiro Kikuchi[b]
Yusuke Furukawa[b] Keiya Ozawa[a]

Divisions of [a]Hematology and [b]Stem Cell Regulation, Jichi Medical University, Shimotsuke, Japan

Multiple myeloma (MM) is a malignant hematopoietic disease that remains incurable. Therapeutic strategies for this disease have been rapidly progressing based on the development of new drugs, including proteasome inhibitors, immunomodulatory agents, antibodies and small molecular compounds such as histone deacetylase inhibitors (HDIs); however, drug resistance remains a major challenge [1]. It is well known that cell adhesion-mediated drug resistance (CAM-DR) occurs when MM cells interact with stromal cells [2]. Specifically, MM cells express surface adhesion receptor molecules which bind with corresponding ligands on stromal cells. Such interaction results in protection of MM cells from the cytotoxic effects of anti-myeloma drugs. We previously found that MM cells express various adhesion molecules, including CD29 (β1-integrin), CD49d (α4-integrin, a subunit of VLA-4), CD54 (intercellular adhesion molecule-1), CD138 (syndecan-1), CD184 (CXC chemokine receptor-4), and CD44. Furthermore, among them CD49d was crucial for CAM-DR to conventional anti-myeloma drugs such as bortezomib and dexamethasone [3]. Thus, it is of great importance to suppress CD49d expression to overcome CAM-DR.

HDI- and DNA-methylating agents show anti-tumor activity by epigenetically re-expressing various genes [4, 5]. These effects might ultimately affect the expression and function of various intracellular molecules, including transcription factors. We therefore hypothesized that these agents influence the expression levels of adhesion molecules in MM cells. To verify this hypothesis, we examined the effect of the HDI romidepsin and DNA-methylating agent azacitidine on the expression levels of CD49d and two other representative adhesion molecules, CD29 and CD138, by flow cytometry analyses in two human MM cell lines, RPMI8226 and U266. Surprisingly and importantly, romidepsin repressed the expression levels of CD49d with statistical significance in both cell lines (fig. 1a, b). Levels of *CD49d* mRNA also markedly decreased after addition of romidepsin, suggesting that romidepsin suppresses *CD49d* expression at the mRNA level (fig. 1c). In contrast, romidepsin had no significant effect on the expression levels of CD29 and CD138 (fig. 1a, b). In RPMI8226 cells, azacitidine also repressed CD49d as well as CD138 (fig. 1a). However, in U266 cells it had no influence on all three adhesion molecules tested, including CD49d (fig. 1b). Since azacitidine failed to disrupt DNA methyltransferases, which are its main targets, in U266 cells [unpubl. data], it is possible that azacitidine had no effect on the pathophysiology of these cells.

0001–5792/13/1321–0001$38.00/0

E-Mail karger@karger.com
www.karger.com/aha

Tadashi Nagai, MD, PhD
Jichi Medical University
3311-1 Yakushiji
Shimotsuke, Tochigi 329-0498 (Japan)
E-Mail t-nagai@jichi.ac.jp

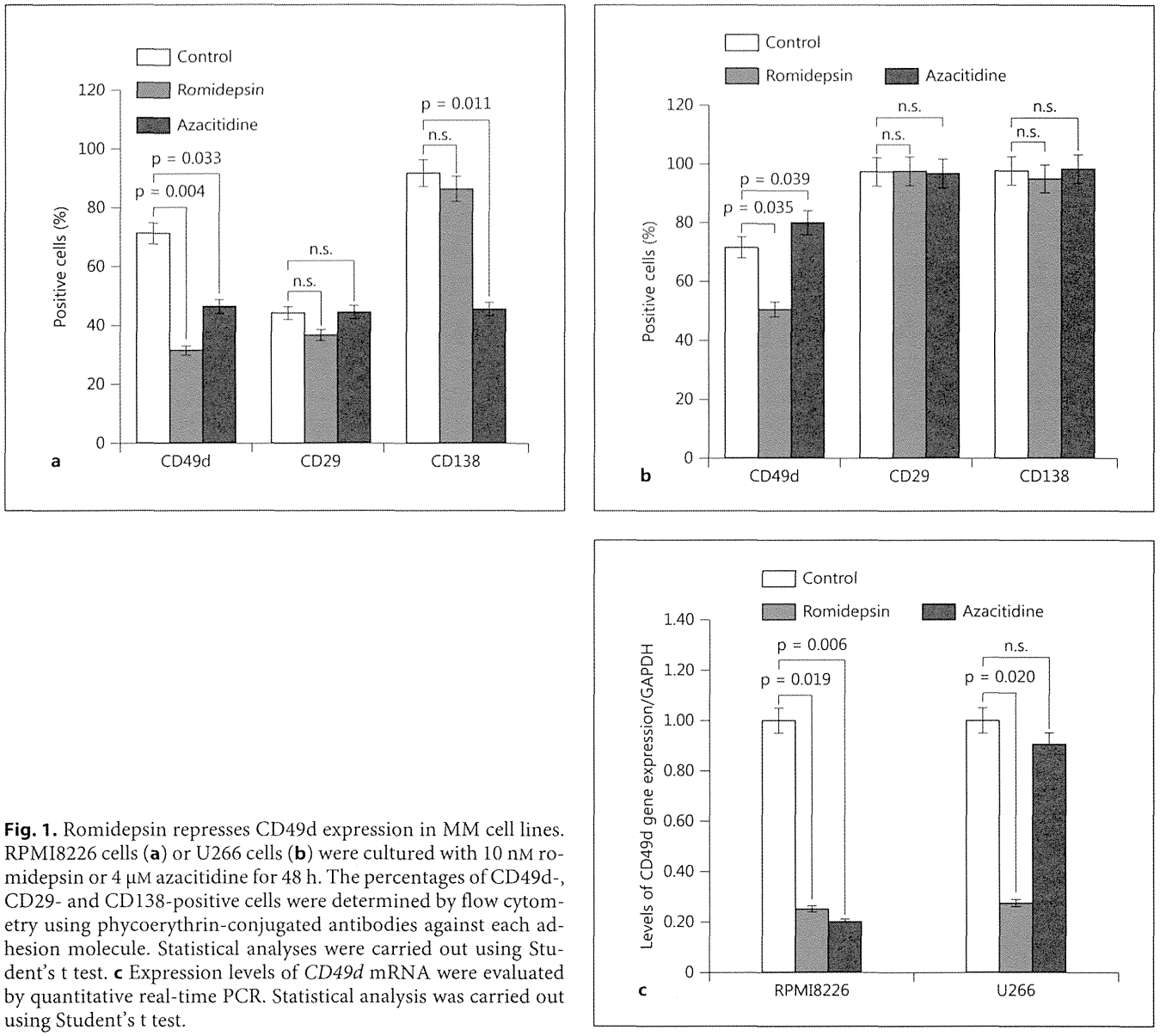

Fig. 1. Romidepsin represses CD49d expression in MM cell lines. RPMI8226 cells (**a**) or U266 cells (**b**) were cultured with 10 nM romidepsin or 4 μM azacitidine for 48 h. The percentages of CD49d-, CD29- and CD138-positive cells were determined by flow cytometry using phycoerythrin-conjugated antibodies against each adhesion molecule. Statistical analyses were carried out using Student's t test. **c** Expression levels of *CD49d* mRNA were evaluated by quantitative real-time PCR. Statistical analysis was carried out using Student's t test.

To clarify whether romidepsin-mediated suppression of *CD49d* expression results in abrogation of CAM-DR to other drugs, we assessed CAM-DR to bortezomib, melphalan and dexamethasone, which are key drugs for MM therapy, using the co-culture system as described previously [3]. In the absence of the stromal cell line UBE6T-7, bortezomib, melphalan and dexamethasone significantly increased the percentage of annexin-V-positive cells, suggesting that these agents effectively induce apoptosis. However, when MM cells were co-cultured with UBE6T-7 cells, induction of apoptosis was suppressed (fig. 2a). We then assessed the reversal of CAM-DR, which was defined as the ratio of annexin-V-positive MM cells in the presence of UBE6T-7 cells to those in the absence of UBE6T-7 cells [3]. As expected, pretreatment of MM cells with romidepsin significantly increased the reversal of CAM-DR to bortezomib, melphalan and dexamethasone in both cell lines (fig. 2b), suggesting that romidepsin effectively overcomes CAM-DR. Consistent with the findings that azacitidine repressed *CD49d* expression in RPMI8226 cells, azacitidine induced the reversal of CAM-DR to these drugs with statistical significance (fig. 2b). In contrast,

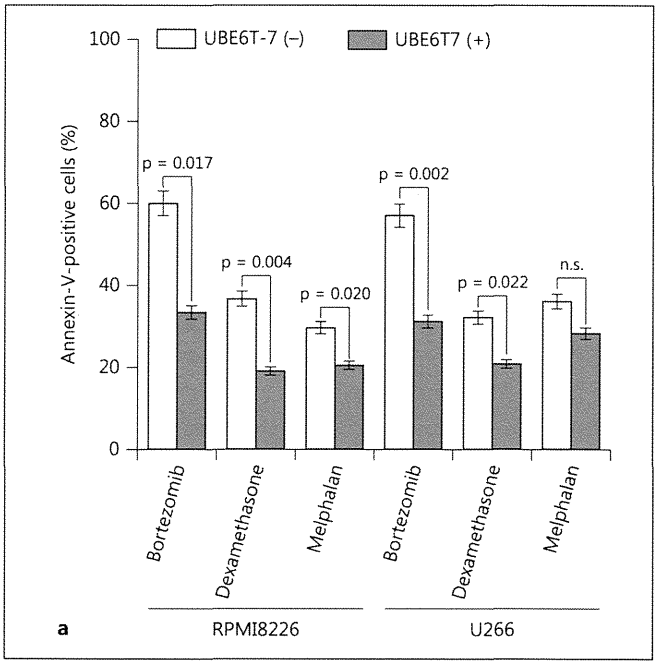

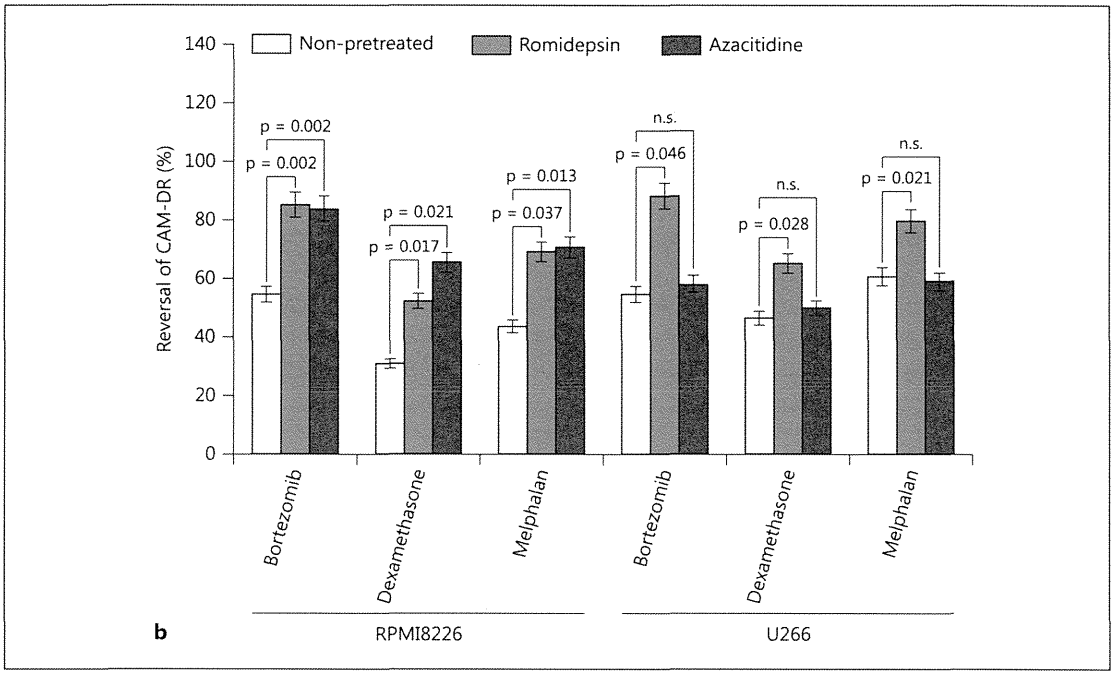

Fig. 2. Romidepsin abrogates CAM-DR to conventional anti-MM drugs. **a** Cells were cultured with 2 nM bortezomib, 10 μM melphalan or 1 μM dexamethasone in the presence or absence of UBE6T-7 cells for 48 h. MM cells were then harvested and stained with annexin-V-FITC. **b** Cells were pretreated with 10 nM romidepsin or 4 μM azacitidine for 24 h and subsequently cultured with 2 nM bortezomib, 10 μM melphalan or 1 μM dexamethasone in the presence or absence of UBE6T-7 cells for a further 48 h. Reversal of CAM-DR was determined as the ratio (%) of annexin-V-positive MM cells in the presence of UBE6T-7 cells to those in the absence of UBE6T-7 cells. Statistical analysis was carried out using Student's t test.

azacitidine had no effect on CAM-DR in U266 cells, the CD49d levels of which were not suppressed by azacitidine.

Histone deacetylases (HDACs) are a class of enzymes that lyse acetyl groups within histones, thus affecting DNA gene expression. They also affect the acetylation status of non-histone proteins such as heat shock protein 90 and α-tubulin, which are involved in the pathophysiology of MM cells. Romidepsin mainly inhibits HDAC1, HDAC2 and HDAC6 [6]. Since HDAC1 and HDAC2 belong to class 1 HDACs, which target histone proteins, it is possible that romidepsin-mediated restoration of gene expressions affects the expression or function of tran-

scription factors that regulate *CD49d* gene expression. Since there are potential binding sites for ETS and WT1 transcription factors on the *CD49d* promoter region [7, 8], it is of great interest to clarify whether romidepsin affects activities of these factors. It is also important to confirm that the *CD49d* expression of MM cells reduces in patients treated with romidepsin.

Interestingly, azacitidine failed to suppress *CD49d* expression, showing no effect on CAM-DR in U266 cells; whereas, just like romidepsin, it abrogated CAM-DR in RPMI8226 cells. U266 are azacitidine-resistant cells, in which its demethylating activity is negated [unpubl. data]; therefore, these results also suggest that restoration of gene expressions due to an improvement of epigenetic status is mainly involved in the repression of *CD49d* in MM cells.

Previous preclinical studies have shown that the combinations of HDIs and bortezomib or other anti-myeloma drugs enhance anti-tumor effects in MM cells [9]. Furthermore, clinical trials have also shown a certain clinical efficacy of combinations of HDIs and other drugs [10, 11]. Combination therapies are promising strategies for the treatment of MM. Interestingly, overexpression of HDAC1 is involved in resistance to bortezomib, and romidepsin overcomes this resistance [12]. The fact that romidepsin overcomes CAM-DR to bortezomib, melphalan and dexamethasone provides additional rationale for an advantage of the combination therapy.

In conclusion, our findings suggest that potentiations of romidepsin and other anti-myeloma drugs, such as bortezomib, melphalan and dexamethasone, are potential therapies for MM in view of overcoming CAM-DR, which is critical for improving the efficacy of anti-myeloma therapy, and might be essential for establishing novel therapeutic strategies to enhance patient outcome or possibly cure the disease.

Acknowledgments

We wish to thank Gary Baley for academic editing. This work is supported in part by grants-in-aid from the Ministry of Education, Culture, Sports, Science and Technology, Japan (25461435).

References

1 Gentile M, Recchia AG, Mazzone C, Lucia E, Vigna E, Morabito F: Perspectives in the treatment of multiple myeloma. Expert Opin Biol Ther 2013;13(suppl 1):S1–S22.

2 Damiano JS, Cress AE, Hazlehurst LA, Shtil AA, Dalton WS: Cell adhesion mediated drug resistance (CAM-DR): role of integrins and resistance to apoptosis in human myeloma cell lines. Blood 1999;93:1658–1667.

3 Noborio-Hatano K, Kikuchi J, Takatoku M, Shimizu R, Wada T, Ueda M, Nobuyoshi M, Oh I, Sato K, Suzuki T, Ozaki K, Mori M, Nagai T, Muroi K, Kano Y, Furukawa Y, Ozawa K: Bortezomib overcomes cell-adhesion-mediated drug resistance through downregulation of VLA-4 expression in multiple myeloma. Oncogene 2009;28:231–242.

4 Marks PA, Xu WS: Histone deacetylase inhibitors: potential in cancer therapy. J Cell Biochem 2009;107:600–608.

5 Christman JK: 5-Azacytidine and 5-aza-2'-deoxycytidine as inhibitors of DNA methylation: mechanistic studies and their implications for cancer therapy. Oncogene 2002;21:5483–5495.

6 Klimek VM, Fircanis S, Maslak P, Guernah I, Baum M, Wu N, Panageas K, Wright JJ, Pandolfi PP, Nimer SD: Tolerability, pharmacodynamics, and pharmacokinetics studies of depsipeptide (romidepsin) in patients with acute myelogenous leukemia or advanced myelodysplastic syndromes. Clin Cancer Res 2008;14:826–832.

7 Rosen GD, Barks JL, Iademarco MF, Fisher RJ, Dean DC: An intricate arrangement of binding sites for the Ets family of transcription factors regulates activity of the alpha 4 integrin gene promoter. J Biol Chem 1994;269:15652–15660.

8 Kirschner KM, Wagner N, Wagner KD, Wellmann S, Scholz H: The Wilms tumor suppressor Wt1 promotes cell adhesion through transcriptional activation of the *α4integrin* gene. J Biol Chem 2006;281:31930–31939.

9 Pei XY, Dai Y, Grant S: Synergistic induction of oxidative injury and apoptosis in human multiple myeloma cells by the proteasome inhibitor bortezomib and histone deacetylase inhibitors. Clin Cancer Res 2004;10:3839–3852.

10 Kaufman JL, Fabre C, Lonial S, Richardson PG: Histone deacetylase inhibitors in multiple myeloma: rationale and evidence for their use in combination therapy. Clin Lymphoma Myeloma Leuk 2013;13:370–376.

11 Richardson PG, Mitsiades CS, Laubach JP, Hajek R, Spicka I, Dimopoulos MA, Moreau P, Siegel DS, Jagannath S, Anderson KC: Preclinical data and early clinical experience supporting the use of histone deacetylase inhibitors in multiple myeloma. Leuk Res 2013;37:829–837.

12 Kikuchi J, Wada T, Shimizu R, Izumi T, Akutsu M, Mitsunaga K, Noborio-Hatano K, Nobuyoshi M, Ozawa K, Kano Y, Furukawa Y: Histone deacetylases are critical targets of bortezomib-induced cytotoxicity in multiple myeloma. Blood 2010;116:406–417.

Exp. Anim. 63(4), 475–481, 2014

—Original—

A Long-term Follow-up Study on the Engraftment of Human Hematopoietic Stem Cells in Sheep

Tomoyuki ABE [1, 2], Yutaka HANAZONO [1, 3], and Yoshikazu NAGAO [2]

[1] *Division of Regenerative Medicine, Center for Molecular Medicine, Jichi Medical University, 3311-1 Yakushiji, Shimotsuke-shi, Tochigi 329-0498, Japan*
[2] *University Farm, Department of Agriculture, Utsunomiya University, 443 Shimokomoriya, Mouka-shi, Tochigi 321-4415, Japan*
[3] *CREST, Japan Science and Technology Agency, 5-3 Yonbancho, Chiyoda-ku, Tokyo 102-8666, Japan*

Abstract: Xenograft models of human hematopoiesis are essential to the study of the engraftment and proliferative potential of human hematopoietic stem cells (HSCs) *in vivo*. Immunodeficient mice and fetal sheep are often used as xenogeneic recipients because they are immunologically naive. In this study, we transplanted human HSCs into fetal sheep and assessed the long-term engraftment of transplanted human HSCs after birth. Fourteen sheep were used in this study. In 4 fetal sheep, HSCs were transduced with homeo-box B4 *(HOXB4)* gene before transplantation, which promoted the expansion of HSCs. Another 4 fetal sheep were subjected to non-myeloablative conditioning with busulfan. Seven of these 8 sheep showed successful engraftment of human HSCs (1–3% of colony-forming units) as assessed after the birth of fetal sheep (5 months post-transplantation), although *HOXB4*-transduced HSCs showed sustained engraftment for up to 40 months. Intact HSCs were transplanted into six non-conditioned fetal sheep, and human colony-forming units were not detected in the sheep after birth. These results suggest that, as compared with mouse models, where the short lifespan of mice limits long-term follow-up of HSC engraftment, the fetal sheep model provides a unique perspective for evaluating long-term engraftment and proliferation of human HSCs.
Key words: engraftment, hematopoietic stem cells, large animal models, long-term follow-up, sheep

Introduction

Animal transplantation models are indispensable for functional assessment of hematopoietic stem cells (HSCs), because reliable *in vitro* surrogate assays for the cells capable of long-term hematopoietic repopulation *in vivo* are currently unavailable [8, 11]. As experimental transplantation of HSCs into humans is ethically unattainable, xenograft models are commonly used for studying engraftment and proliferative potential of human HSCs *in vivo*. Several xenogeneic transplantation models have been studied, of which immunodeficient mice [5–7, 9, 15] and fetal sheep [31] are advantageous because of their immunologically naive state. Human HSCs can readily engraft and generate progeny in these animals. Although immunodeficient mice have gained the broadest application in laboratory research due to the ease of access and handling of animals, humans and mice show distinct differences, especially in lifespan and body size, which are relevant to HSC transplantation. The reconstitution of human hematopoiesis in mice allows for observation for 1–2 y after serial transplantation [10, 16, 29]; however, execution of the procedure requires a large number of mice (Fig. 1).

The aim of this study was to examine whether the transplantation of human HSCs into fetal sheep could

(Received 22 April 2014 / Accepted 28 May 2014 / Published online in J-STAGE 22 July 2014)
Address corresponding: Yutaka Hanazono (MD, PhD), Division of Regenerative Medicine, Center for Molecular Medicine, Jichi Medical University, 3311-1 Yakushiji, Shimotsuke-shi, Tochigi 329-0498, Japan

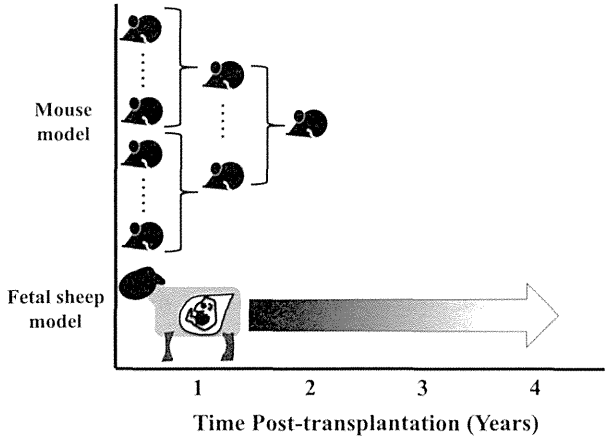

Fig. 1. Long-term assessment of human HSCs *in vivo*. In immunodeficient mice, although serial transplantation is an approach to evaluate the long-term assessment of human hematopoietic stem cells (HSCs), a large number of mice are required for the following transplantation. In contrast in sheep, the long-term assessment can be achieved in single animals. It is possible to conduct repeated bleeding and evaluation of samples at desired intervals over long periods without serial transplantation in sheep.

allow long-term engraftment of the cells in the sheep after birth. Long-term assessment of human HSCs in sheep can be performed because the large size and long lifespan of sheep allow repeated sampling of bone marrow (BM) in individual animals at desired intervals for long periods of time [1, 24, 31]. Here we report sustained engraftment of human HSCs in sheep for up to 40 months post-transplantation as assessed by clonogenic assays of the BM.

Materials and Methods

Animals

Pregnant Suffolk ewes (Japan Lamb, Hiroshima, Japan) were bred at Jichi Medical University and at Utsunomiya University Farm. All experiments in this study were performed in accordance with the Jichi Medical University Guide for Laboratory Animals and the Utsunomiya University Guide for Experimental Animals.

Graft preparation

Human cord blood (CB) was supplied by the RIKEN BioResource Center Cell Bank (Ibaraki, Japan). Human CB $CD34^+$ cells, used as hematopoietic stem cells (HSCs), were isolated by immunomagnetic separation using an anti-human CD34 microbeads kit (Miltenyi Biotech, Auburn, CA, USA) according to the manufacturer's instructions. In a protocol (4 out of the 14 CB samples), namely *HOXB4* protocol, human CB $CD34^+$ cells were transduced before transplantation with a polymerase gene-defective Sendai virus vector (DNAVEC Corp., Ibaraki, Japan) that transiently expressed the human *HOXB4* gene (GenBank accession No. NM 024015). The *HOXB4* gene provided a selective growth advantage to transduced HSCs *in vivo* [4, 25, 26, 32]. The transduction was conducted by culturing the cells for 4 days in the presence of 100 ng/ml recombinant human (rh) stem cell factor (SCF), rh Flt3 ligand (both from R&D Systems, Minneapolis, MI, USA) and rh thrombopoietin (Kyowa Hakko-Kirin Co., Ltd., Tokyo, Japan) [1].

In utero transplantation (IUT)

The cells were transplanted into the liver of fetal sheep at 45 to 49 days of gestation (full term, 147 days). The procedures of IUT were described previously [17]. In another protocol (the BU protocol), some fetuses (4 out of the 14 sheep) received busulfan (BU, Wako Pure Chemical Industries Ltd., Osaka, Japan) via the dams intravenously at 3 mg/kg (calculated based on maternal body weight) 6 days before transplantation [2]. BU is often administered to patients as a conditioning agent before HSC transplantation [3, 21].

Colony-forming unit (CFU) assay

CB $CD34^+$ cells used for transplantation or sheep bone marrow (BM) cells post-transplantation were subjected to CFU assay. Briefly, cells were plated in a 35-mm petri dish with 1 ml of MethoCult GF^+ H4435 (StemCell Technologies, Vancouver, BC, Canada) containing SCF, granulocyte colony-stimulating factor (G-CSF), granulocyte-macrophage CSF, interleukin (IL)-3, IL-6 and erythropoietin, which were recombinant human products and purchased from StemCell Technologies. The culture conditions equivalently support the growth of ovine as well as human CFUs, and thus no difference in the efficiency of colony formation between ovine and human hematopoietic cells was observed in this assay [24]. After incubation at 37°C with 5% CO_2 for 14 days, colonies containing more than 50 cells were counted under an inverted light microscope [1, 2]. Statistical significance of the difference in colony numbers was determined by the ANOVA-test.

Table 1. Long-term engraftment in sheep after in-utero transplantation of human hematopoietic stem cells

Protocols	Animal no.	In utero transplantation			Engraftment (% of human CFUs)[a]				
		Gestational day of transplant (Full term: 147 days)	Number of transplanted cells per fetus ($\times 10^5$)	Number of transplanted $CD34^+$ cells per fetus ($\times 10^5$)	5 months post IUT	15–17 months post IUT	20–25 months post IUT	40 months post IUT	58 months post IUT
HOXB4[b]	Y705-1	49	5.2	3.8	0.0	0.0	0.0	-	
	Y705-2	49	4.5	4.5	1.1	2.2	2.2	2.2	0.0
	Y271-1	49	3.2	2.9	3.3	1.1	0.0	-	
	Y271-2	49	8.9	7.6	2.2	0.0	0.0	-	
BU[c]	Y940-1	48	20.0	17.5	1.1	-[e]			
	Y940-2	48	20.1	13.8	1.1	-	0.0	-	
	Y1061-1	48	7.2	2.8	2.2	0.0	-		
	Y1061-2	48	10.7	5.8	3.3	0.0	-		
Non-treatment[d]	Y1018-1	49	23.6	17.8	0.0	-			
	Y1018-2	49	15.5	12.0	0.0	-			
	Y973	45	8.6	5.6	0.0	-			
	Y936	47	7.3	5.4	0.0	-			
	W110	48	17.7	13.7	0.0	-			
	Y955	48	13.3	10.1	0.0	-			

[a] Percentage of human CFUs was calculated by dividing the number of CFUs positive for the human-specific *β2-microglobulin* gene sequence by the total number of CFUs being analyzed in the bone marrow. [b] In the *HOXB4* protocol, human $CD34^+$ cells transduced with *HoxB4* were transplanted into non-con ditioned fetal sheep [1]. [c] In the BU protocol, BU was administered 6 days before IUT of non-transduced human $CD34^+$ cells [2]. [d] In the non-treatment protocol, non-transduced human $CD34^+$ cells were transplanted into non-conditioned fetal s heep [1, 2]. [e] Sheep Y940-1 unexpectedly died from an accident during the procedures of bone marrow aspiration. CFU, colony-forming unit; BU, busulfan; IUT, in utero transplantation.

Assessment of human engraftment

To evaluate the engraftment of human cells, BM was aspirated from the iliac bone of lambs using a 13-gauge biopsy needle (Jamshidi, CareFusion, San Diego, USA), under local anesthesia with 2% lidocain (Xylocaine, AstraZeneca, Tokyo, Japan). BM cells were harvested by removing red blood cells with ACK lysis buffer (155 mM NH_4Cl, 100 mM $KHCO_3$, and 1 mM EDTA) (Wako Pure Chemical Industries, Ltd.). *In vitro* colony formation assay of sheep BM cells after transplantation was conducted as described above (in the section of *CFU assay*). Each colony was derived from a single human or sheep hematopoietic progenitor cell. DNA of each colony was subjected to polymerase chain reaction (PCR) to identify human colonies [24]. First, each colony was plucked into 50 μl of distilled water and digested with 20 μg/ml proteinase K (Takara, Shiga, Japan) at 55°C for 2 h, followed by 99°C for 10 min, to extract DNA. Each DNA sample (5 μl) was used for a nested PCR to identify the human β2-microglobulin–specific sequences [1, 2]. The outer primer set was 5′-CAGGTTTACTCACGTCATCCAG-3′ and 5′-GGTTCACACGGCAGGCATACTC-3′, and the inner primer set was 5′-GTCTGGGTTTCATCCATCCG-3′ and 5′- GGTGAATTCAGTGTAGTACAAG-3′. The amplification conditions for the outer PCR were 95°C for 30 s, 58°C for 30 s, and 72°C for 30 s for 25 cycles. The outer PCR products were purified using a QIA quick PCR purification kit (Qiagen, Chatsworth, CA, USA). The amplification conditions for the inner PCR were 95°C for 30 s, 58°C for 30 s, and 72°C for 30 s for 30 cycles. Simultaneous PCR for the β-actin sequence was also performed to verify the DNA amplification of each sample. The primer sequences of either humans or sheep were 5′-GTCACCCACACTGTGCCCATCTACG-3′ and 5′-GCCATCTCCTGCTCGAAGTC-3′. The amplification conditions were 94°C for 30 s, 55°C for 30 s, and 72°C for 30 s for 40 cycles. The amplified human β2-microglobulin (133 bp) and *β*-actin (209 bp) products were resolved by 2% agarose gel and visualized by ethidium bromide staining. The engraftment efficiency of human hematopoietic cells was expressed as the ratio of the number of human-derived colonies to the total number of colonies.

Results

Frozen human cord blood (CB) was obtained from RIKEN Cell Bank. The cells were thawed, and a range of $2.8 \times 10^5 - 17.8 \times 10^5$ of $CD34^+$ cells were isolated